Science of the Total Environment 686 (2019) 737–752

Contents lists available at ScienceDirect

Science of the Total Environment

journal homepage: www.elsevier.com/locate/scitotenv

African dust and air quality over Spain: Is it only dust that matters?

X. Querol [a,*], N. Pérez [a], C. Reche [a], M. Ealo [a], A. Ripoll [a], J. Tur [a], M. Pandolfi [a], J. Pey [b], P. Salvador [c], T. Moreno [a], A. Alastuey [a]

[a] Institute of Environmental Assessment and Water Research IDAEA-CSIC, C/Jordi Girona 18-26, Barcelona 08034, Spain
[b] ARAID, Instituto Pirenaico de Ecología (IPE-CSIC), 50059 Zaragoza, Spain
[c] Department of Environment, Joint Research Unit Atmospheric Pollution CIEMAT-CSIC, Madrid 28040, Spain

HIGHLIGHTS

- African dust transport affects air quality of Spain during 9 (NW Iberia) to 31 (Canary Islands)% of days.
- PM10 & PM2.5 levels increase by 9 to 29 and 5 to 29 μg/m^3 PM10 and PM2.5 from NW Iberia to the Canary Islands.
- PM speciation shows that this increase is due to mineral dust and anthropogenic PM co-transported or locally accumulated.
- For epidemiological studies the two fractions have to be studied with regards the evaluation of possible health effects.

GRAPHICAL ABSTRACT

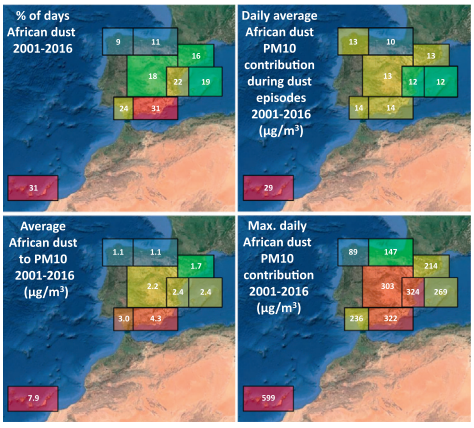

ARTICLE INFO

Article history:
Received 15 February 2019
Received in revised form 16 May 2019
Accepted 23 May 2019
Available online 24 May 2019

Editor: Pavlos Kassomenos

Keywords:
PM10
PM2.5
Desert dust
Geochemistry
Aerosols

ABSTRACT

The 2001–2016 contribution of African dust outbreaks to ambient regional background PM10 and PM2.5 levels over Spain, as well as changes induced in the PMx composition over NE Spain in 2009–2016, were investigated. A clear decrease in PMx dust contributions from the Canary Islands to N Iberia was found. A parallel increase in the PM2.5/PM10 ratio (30% in the Canary Islands to 57% in NW Iberia) was evidenced, probably due to size segregation and the larger relative contribution of the local PMx with increasing distance from Africa.

PM1–10 and PM2.5–10 measured in Barcelona during African dust outbreaks (ADOs) were 43–46% higher compared to non-ADO days. The continental background contribution prevailed in terms of both PM1–10 and PM2.5–10 during ADO days (62 and 69%, respectively, and 31 and 27% for non-ADO days). The relative contributions of Al_2O_3/Fe_2O_3/CaO to PMx fraction showed that Al_2O_3 is a suitable tracer for African dust in our context; while CaO at the urban site is clearly affected by local resuspension, construction and road dust, and Fe_2O_3 by dust from vehicle brake discs. The results also provide evidence that PM increases during ADOs are caused not only by the mineral dust load, but by an increased accumulation of locally emitted or co-transported anthropogenic pollutants as compared with non-ADO days. Possible causes for this accumulation are discussed. We recommend that further epidemiological studies should explore independently the potential effects of mineral dust and the anthropogenic PM during ADOs, because, at least over SW Europe, not only mineral dust affects the air quality during African dust episodes.

* Corresponding author.
E-mail address: xavier.querol@idaea.csic.es (X. Querol).

https://doi.org/10.1016/j.scitotenv.2019.05.349

1. Introduction

Arid regions contribute very large loads to the global atmospheric aerosols, with around $1.5 \cdot 10^9$ tons/year of dust being emitted into the troposphere (Textor et al., 2006; Huneeus et al., 2011; Ginoux et al., 2012; Kok et al., 2017). Among these regions, N Africa (Sahara and Sahel) is the largest contributor, with almost 50% of the global dust emissions (around 0.8 10^9 tons/yr; Prospero et al., 2002; Washington et al., 2003; Walker et al., 2009; Ginoux et al., 2010, 2012; Huneeus et al., 2011; Varga, 2012).

Dust emitted in N Africa is significally transported towards the Caribbean region (Prospero et al., 2002; Prospero and Lamb, 2003; Ginoux et al., 2012; and references therein); however, under specific meteorological scenarios, dust is also transported towards continental Europe and the Mediterranean region (e.g., Moulin et al., 1997, 1998; Rodriguez et al., 2001; Escudero et al., 2005; Querol et al., 2009; Varga, 2012; Pey et al., 2013).

Bergametti et al. (1989a, 1989b), Dayan et al. (1991) and Kubilay and Saydam (1995) reported on the influence of African dust outbreaks (ADOs) on ambient levels of total suspended particles (TSP). By assessing air quality around a large coal-fired power plant, Querol et al. (1998a) reported that a number of annual exceedances of the EU daily PM10 air quality standard in Spain were due to African dust contributions. Since then, many subsequent studies (e.g., Querol et al., 1998b, 2009; Rodriguez et al., 2001; Viana et al., 2002; Escudero et al., 2005, 2007a, 2007b; Pey et al., 2013; Pandolfi et al., 2014a; among others), have demonstrated the impact of ADOs on the air quality over Spain.

Querol et al. (2009) and Pey et al. (2013) reported on the occurrence of ADOs over the whole Mediterranean Basin and calculated frequencies of occurrence of 30–37% of the days in the southern parts of the Basin to <20% for the northern ones. There was also an increasing gradient of ADO frequency from the western (23%) to the eastern (31%) regions. Furtermore, the western part has a lower occurrence of severe episodes (daily dust averages over 100 μg/ m^3 PM10). Overall, African dust emerged as the largest PM10 source in regional background southern sites of the Mediterranean. This contribution ranged from 35 and 25% of annual PM10 means in south-eastern and south-western regions, respectively, to 10% in the northern ones, with seasonal peak contributions to PM10 up to 80% of the total mass in the highest ADO influenced regions. Achilleos et al. (2014) reported for Nicosia, Cyprus, that PM10 concentrations during desert dust storms reached an average of 100 μg/m^3, but also that ADOs were responsible for a small fraction of the exceedances of the daily PM10 limit. Matthaios et al. (2016) reported that 53% of exceedances of the EU daily PM10 limit value recorded in Greece were mainly caused by local pollution sources, whereas 47% of these were caused by ADOs, and that the averaged PM10 for these exceedance days reached 65 and 100 μg/m^3, respectively.

A number of studies have evaluated the health effects associated with ADOs in Spain (Pérez et al., 2008a, 2012; Jiménez et al., 2010; Tobías et al., 2011; Díaz et al., 2012, 2017; Reyes et al., 2014), reporting that daily mortality and morbidity increase during ADOs when compared with non-dust days. In some of these studies, a higher increase in risk of premature mortality with the growth of PM10 (and PM2.5–10) concentrations during ADOs (compared with non-dust days) was evidenced. In order to study the causes of this higher possible toxicity, Pandolfi et al. (2014a) evaluated the effect of ADOs on the concentrations of a number of pollutants and on the mixing layer height (MLH) in Barcelona. A marked thinning of the MLH during ADOs compared with non-dust days was found, and it was demonstrated that PM1 and local gaseous pollutants concentrations also increased relatively during ADOs. Thus, the ADOs in Barcelona caused a reduction in the MLH with a consequent accumulation of local anthropogenic pollutants, which likely explains the increased harmful health effects of PMx.

Our study aims at evaluating the impact of ADOs on the concentrations of PM2.5 and PM10 across Spain during the 2001–2016 period, followed by a more specific study on the effects of ADOs on the concentrations of locally- and regionally-emitted pollutants in NE Spain, such as BC and UFP, as well as on PMx levels and speciation, by comparing 2009–2016 measurements performed at three (urban, regional and continental) background stations in and around Barcelona.

2. Methodology

2.1. Estimation of African dust contributions to PM10 and PM2.5 over Spain

2.1.1. PM measurements

In order to evaluate ADOs across Spain and assess their impact on PM10 and PM2.5 levels, the 2001–2016 daily averaged PM data from 44 remote, regional and sub-urban background air quality monitoring sites spread across Spain (including the mainland and the Balearic and Canary Islands, Fig. 1) were used. This is a network of existing air quality monitoring stations from regional governments and EMEP to which we have access to the data, in most cases online access. Details on the locations of the air quality monitoring sites and data used are reported in Table S1 and a file included as supplementary information. Different techniques were used to determine PM concentrations: gravimetric determinations at the European Monitoring and Evaluation Programme (EMEP) sites and real-time PM instruments (BETA, TEOM and optical counters, at the rest of the sites). Real-time concentrations were corrected against the gravimetric concentrations according to the current European air quality monitoring standards (EN-12341 and EN-14907). Since only official data (supplied by Member States of the European Environmental Agency and EMEP programme databases after different validation steps) are used in this work, data quality is guaranteed.

Our selection of reference sites has limitations. First a few stations are not remote or regional background sites but are sub-urban. In the latter the anthropogenic load of PM10 and PM2.5 is higher and this might dilute the relative contribution of African dust to averaged PMx levels, but we believe this is not affecting to the calculation of the dust load. On the other hand the altitude of the monitoring sites might vary from close to sea level to the highest one in the Pre-Pyrenees (Montsec 1568 m a.s.l.). This might affect the comparability of dust loads across Spain because dust might preferentially be transported at high altitudes and accordingly affect with higher intensity to mountain sites (Querol et al., 2009; Pey et al., 2013).

2.1.2. Identification of the African dust influence and quantitative determinations of the PM dust contributions

The methodology used to identify ADOs and quantify their impact on PMx has been described in detail elsewhere (Rodríguez et al., 2001; Escudero et al., 2005, 2007a, 2007b; Querol et al., 2009; Pey et al., 2013; Salvador et al., 2013, 2014). This methodology has been officially accepted by the European Commission for reporting on natural contributions to ambient PM levels over Europe (EC, 2011). It consists, first of all, of the identification of the ADOs day by day at every specific location, by using different model outputs and meteorological information (such as the NCEP/NCAR: http://www.esrl.noaa.gov/psd/data/composites/hour/; NMMB-BSC-dust model, https://dust.aemet.es/forecast/nmmb-bsc-dust-forecast-sconc; NAAPS-NRL model, http://

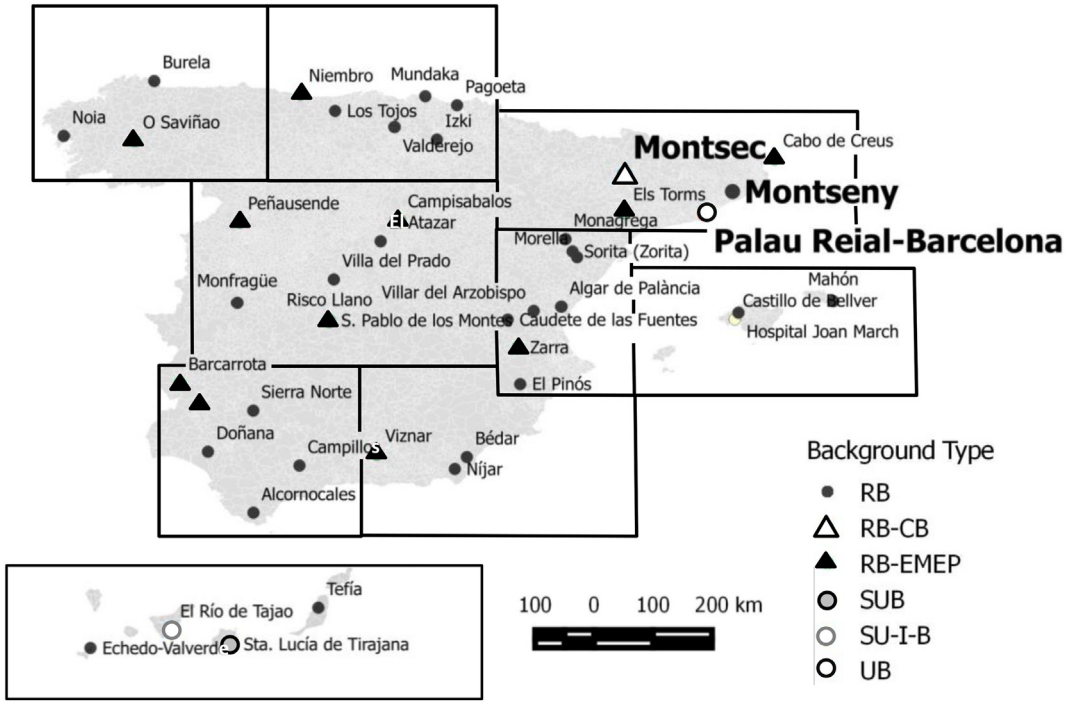

Fig. 1. Location of the PM monitoring stations and the three supersites in NE Spain (Montseny, Montsec and Palau Reial-Barcelona). The regions marked correspond to the ones differentiated in Figs. 2 and 3.

www.nrlmry.navy.mil/aerosol/; SKIRON dust simulations, http://forecast.uoa.gr/dustindx.php; BSC-DREAM8b, http://www.bsc.es/ess/bsc-dust-daily-forecast; HYSPLIT air mass back-trajectories, https://ready.arl.noaa.gov/HYSPLIT.php; among others) and using surface PM10 and PM2.5 measurements from the monitoring network of regional background sites described above.

In the second step, a statistical methodology is applied to the PMx data series registered at regional background sites in order to obtain quantitative estimates of the African dust loads to daily PM10 and PM2.5 concentrations during ADOs. Once we identified the ADO days, using the PMx data sets from the remote-regional background-reference sites, we excluded the PMx concentrations for each of them and we calculated, also for each ADO day, the moving (30 days) 40th percentile, with the ADO day being in position 15/30. This 40th percentile value is considered equivalent to the regional background without ADO and this is subtracted to the averaged PMx levels for the respective ADO day to obtain the net dust contribution. We selected the 40th percentile as a result of sensitivity analysis by comparing the method with PM10 mineral dust obtained with chemical analysis for different sites over the Iberian Peninsula.

2.2. PM10, PM2.5, PM1, BC and UFP in NE Iberia

2.2.1. Monitoring sites

PM10, PM2.5, PM1, UFP and BC concentrations were measured at three air quality and climate research monitoring supersites located in NE Iberia (Fig. 1) representing the urban background of Barcelona (UB, 70 m a.s.l.), the regional background (RB) approximately 40 km to the NE of the city (Montseny, MSY, 720 m a.s.l., ACTRIS-GAW) and the continental background (CB) at the high-altitude Montsec station, located approximately 175 km from Barcelona in the Pre-Pyrenean Range (MSA, 1592 m a.s.l., ACTRIS-GAW). These stations integrate the monitoring network of the Environmental Geochemistry and Atmospheric Research Group (EGAR) and are operated in collaboration with the regional government of Catalonia (Departament de Territori i Sostenibilitat, Generalitat de Catalunya). Data availability starts in 2002 for the RB site, 2003 for the UB site, and 2009 for the CB site. Thus, we have focused our study in NE Spain on the period 2009–2016.

The meteorology of this region is in between the Atlantic and the Mediterranean influences. In winter the location of the Azores high favours the westerly trade winds leading to the replacement of the existing air masses by clean Atlantic air masses. During the warm seasons the typical Mediterranean climate governs the atmospheric dynamics of this area, with long dry periods, sporadic but occasionally heavy rains. The weak pressure gradients in summer result in local circulations dominating the atmospheric dynamics with the consequent accumulation of pollutants (Millán et al., 1997). The MSA site, a high altitude emplacement located in a low-density populated region, isolated from large urban and industrial agglomerations, is under free tropospheric (FT) influence most of the time, although it is exposed to regional pollutants during the summer time and/or under the influence of mountain breezes, and it is affected by trans-boundary incursions of natural and anthropogenic aerosols from Europe and N Africa (Ripoll et al., 2014, 2015; Minguillón et al., 2015; Ealo et al., 2018). The MSY station is located on the upper walls of a valley extending perpendicularly from the Catalan Pre-Coastal ranges to the coast, in a densely forested area, 50 km to the N-NE of the Barcelona urban area, and 25 km from the Mediterranean coast. The site is relatively far from urban and industrial areas, but it can be affected by anthropogenic emissions transported from populated and industrialised areas under specific meteorological conditions. Out of the scenarios dominated by synoptic winds, and especially in spring and summer, pollutants accumulated in the valley under anticyclonic atmospheric conditions can be transported to the MSY site by upslope and sea breezes activated by the sun radiation at midday (Pérez et al. 2008b, 2008c; Pandolfi et al., 2014b, Ealo et al., 2018).

The UB site is located in Barcelona, a densely populated area, affected by emissions from traffic, industry and with one of the major harbours

in the Mediterranean. In addition to the aforementioned meteorological processes, dispersion of pollutants in the city is governed by the sea breezes (Pérez et al., 2010; Minguillón et al., 2016).

2.2.2. Online measurements

Measurements of aerosol particle variables were performed simultaneously at the three sites by using the same methodology. Ambient air concentrations of PMx were obtained using particle optical counters (GRIMM spectrometers) (Table S2). These measurements were corrected by comparison with simultaneous gravimetrically-determined PM values (with factors usually varying from 1.1 to 1.3). To this end, PM10, PM2.5 and PM1 24 h samples were collected every four days by using collocated high-volume samplers (30 m^3/h, DIGITEL and MCV), provided with quartz microfiber filters (Munktell and Pallflex). The total number of filters collected during the period considered is shown in Table S1. Concentrations of equivalent black carbon (eBC) were measured with Multiangle Absorption Photometers (MAAP, Thermo Scientific) using the mass absorption cross-section coefficients provided by the manufacturer. Levels of UFP were measured using Condensation Particle Counters (CPC, TSI; see models and size ranges in Table S2).

2.2.3. Chemical speciation of PM10, PM2.5 and PM1

A large number of samples of PM10, PM2.5 and PM1, obtained simultaneously every 4 days at the UB, RB and CB (only PM10 and PM1 at the latter), were chemically analysed. To this end, we analysed 2340, 2012 and 1144 filter samples at the three sites, respectively (Table S2), following the methodology proposed by Querol et al. (2001). This method consists of leaching one-fourth of the filter and analysing the soluble ions via ion chromatography, with the exception of NH_4, for which a specific electrode was used; the HF:HNO_3:$HClO_4$ digestion of another one-half of the filter, and the subsequent analysis of around 40 major and trace elements by inductively coupled optical emission spectrometry and inductive mass spectrometry; and the analysis of organic and elemental carbon (OC and EC) by means of the thermo-optical-transmission method and using the EUSAAR2 protocol. Concentrations were blank corrected, and certified standards were analysed following the same methodology.

2.3. Back-trajectory analysis

We determined the daily backward air mass trajectories for a central site of each of the areas into which we divided the Spain territory for the ADOs study (see Fig. 1). To this end, we used the HYSPLIT atmospheric transport and dispersion model (Stein et al., 2015; Rolph et al., 2017) to obtain 120 h back-isentropic trajectories at midday (12 UTC), at three different heights (750, 1500 and 2500 m a.g.l.) using GDAS1 meteorological data. We distinguished the following daily air mass origins according to the results: the N, NW, SW and W Atlantic air masses (NA, NWA, SWA and WA) as well as the Mediterranean (MED), European (EU), N African (ADO), Regional (REG) and Winter Anticyclonic Episode (WAE) air masses. The latter two represent those episodes in which trajectories from 5 previous days do not exceed an area of 500 km around Iberia in summer-spring (REG) or winter-autumn (WAE). The spatial limits of the origins of the above air masses are shown in Fig. S1.

2.4. Determination of the height of the mixing layer at midday

Pandolfi et al. (2014a) demonstrated that during the most intensive ADOs in Barcelona the MLH was markedly reduced and this caused an accumulation of local pollution; thus we considered relevant to include here an analysis of the MLH in Barcelona for the study period. The MLH was calculated by means of the simple parcel method (Holzworth, 1964), i.e., by using the vertical profiles of pressure and temperature from radiosondes (model Vaisala RS92-SGP) launched at 12:00 UTC from a radio-sounding system run by the Physics Department of the University of Barcelona. With this method, the MLH is taken as the equilibrium level of an air parcel, with the potential temperature (calculated from the vertical profiles of temperature and pressure) calculated at ground level. The parcel method is highly effective for the determination of the MLH height in the case of marked inversions, which are usually observed at midday when convective activity is high. This method has already been successfully applied to radio-sounding data collected in Barcelona, as reported in Pandolfi et al. (2013, 2014a, 2014b). Based on this method, a total of >2000 MLH were determined daily at midday during the period 2009–2016.

3. Results and discussion

3.1. Occurrence of ADOs over Spain

3.1.1. Frequency of ADOs and contributions to levels of PM10 and PM2.5

A number of statistical parameters that reflect the influence of ADOs on the PM10 and PM2.5 ambient concentrations in the differentiated regions of Spain are shown in Tables S3 and S4 and Figs. 2 and 3. The results indicate that the proportion of days with PM10 levels affected by ADOs during 2001–2016 ranges from 31% in the Canary Islands and SE Iberia to 9 and 11% in NW and N Iberia, respectively (Fig. 2a and Table S3a). The remaining areas of the Iberian Peninsula and the Balearic Islands are affected by ADOs from 16 to 24% of the days.

The average dust contributions to PM10 during ADO days reached 29 μg/m^3 in the Canary Islands (with a daily maximum of 599 μg/m^3), 10 and 14 μg/m^3 in N and S Iberia, respectively (with daily maxima of 89 and 322 μg/m^3, respectively), and from 12 to 13 μg/m^3 in Central, NW, E, NE Iberia and the Balearic Islands (with maxima from 147 to 324 μg/m^3) (Fig. 2b and c and Table S3a). For PM2.5, the averaged concentrations reached 9 μg/m^3 for the Canaries, 6–7 μg/m^3 for the whole of Iberia and 4 μg/m^3 for the Balearic Islands (in this case, with relative low data availability, 2012–2016), with daily maxima of 103–114 μg/m^3 in the Canary Islands, NE, SE and Central Iberia and of 32–66 μg/m^3 in the remaining study areas (Fig. 3a and c and Table S4a).

Average contributions of African dust to the annual means of the PM10 and PM2.5 levels (Figs. 2f and 3f and Table S3b and 4b) are close to 32 and 35%, respectively, in the Canary Islands, 17–21 and 15–16% in SW and SE Iberia, 18 and 13% in Central and E Iberia, and 8–10 and 7–8% in the other regions (NE, NW and N Iberia). In the Balearic region, the contributions are relatively low when compared with the neighbouring E Iberia region (12 and 3%, respectively). This difference is probably due to the fact that the reference sites in the Balearic regions are close to urban areas and therefore affected by local anthropogenic emissions, thus yielding high annual bulk PM10 levels when compared to the E Iberia sites (20 and 13 μg/m^3, respectively). Furthermore, high mountain sites over Iberia, including Montsec, Campisábalos, Viznar, Riscollano and Morella (1535 to 1150 m a.s.l.), are affected more by dust transported at relatively high altitudes, something that occurs recurrently in summer (Querol et al., 2009; Pey et al., 2013).

It is remarkable that the percentage of PM2.5 in PM10 for the average dust loads during ADO days increases with the distance to the African continent (Fig. 3b), with the PM2.5/PM10 ratio of the dust load contribution reaching 30–36% in the Canary and Balearic Islands, 41–44% in SW, SE and Central Iberia, and 47–57% in E, NE, N and NW Iberia. This result is probably a consequence of the higher deposition rates of the particles with bigger sizes along the air masses transport, but also the increased proportion of local/regional PMx (with finer PM size) as the distance from Africa increases.

We applied the Mann-Kendall test to the frequency and intensity of ADOs in the different study regions and we did not obtain clear trends on both parameters in any of the time series we worked in the present study.

In summary, a clear decrease in PM10 and PM2.5 dust contributions is observed from the maxima of the Canary Islands to N Iberia as the

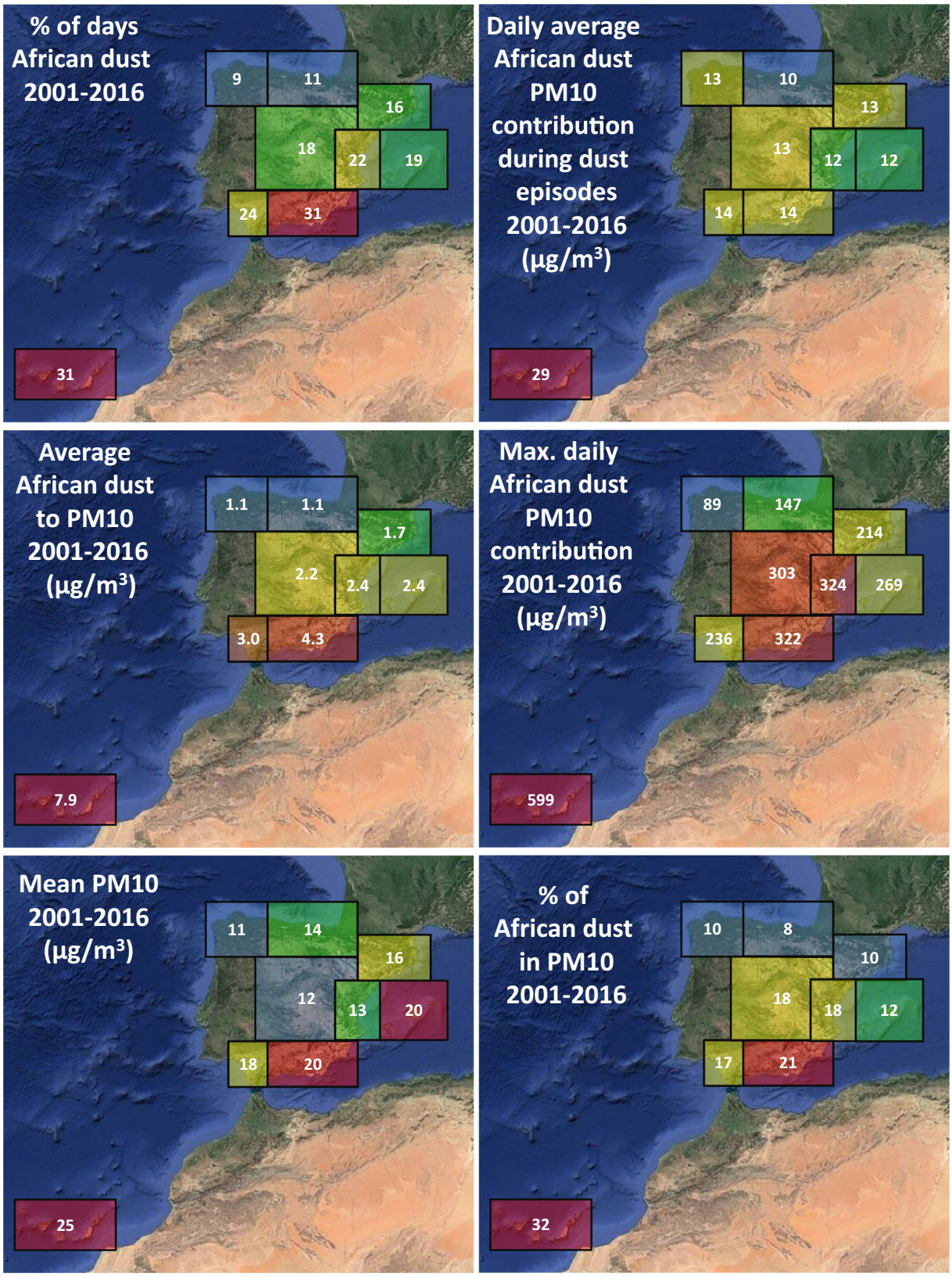

Fig. 2. a) 2001–2016 averaged percentage of days with African dust outbreaks for the 9 study regions of Spain. b) Daily average of African dust contribution to PM10 during dust episodes (µg/m^3). c) Average African dust to annual PM10 means (µg/m^3). d) Maxima daily African dust PM10 contribution (µg/m^3). e) Mean PM10 (µg/m^3). f) Percentage of African dust to the annual PM10 means. Values correspond to averages of annual means of daily levels.

distance to Africa increases. The highest ADO impact in the Canary Islands is due to its proximity to the African continent and the major easterly transport of the air masses in this area of the northern hemisphere (Prospero et al., 2002; Ginoux et al., 2012). The similarly high proportion of ADOs recorded in SE Iberia is also attributable to the proximity of the region to the African continent but also to the

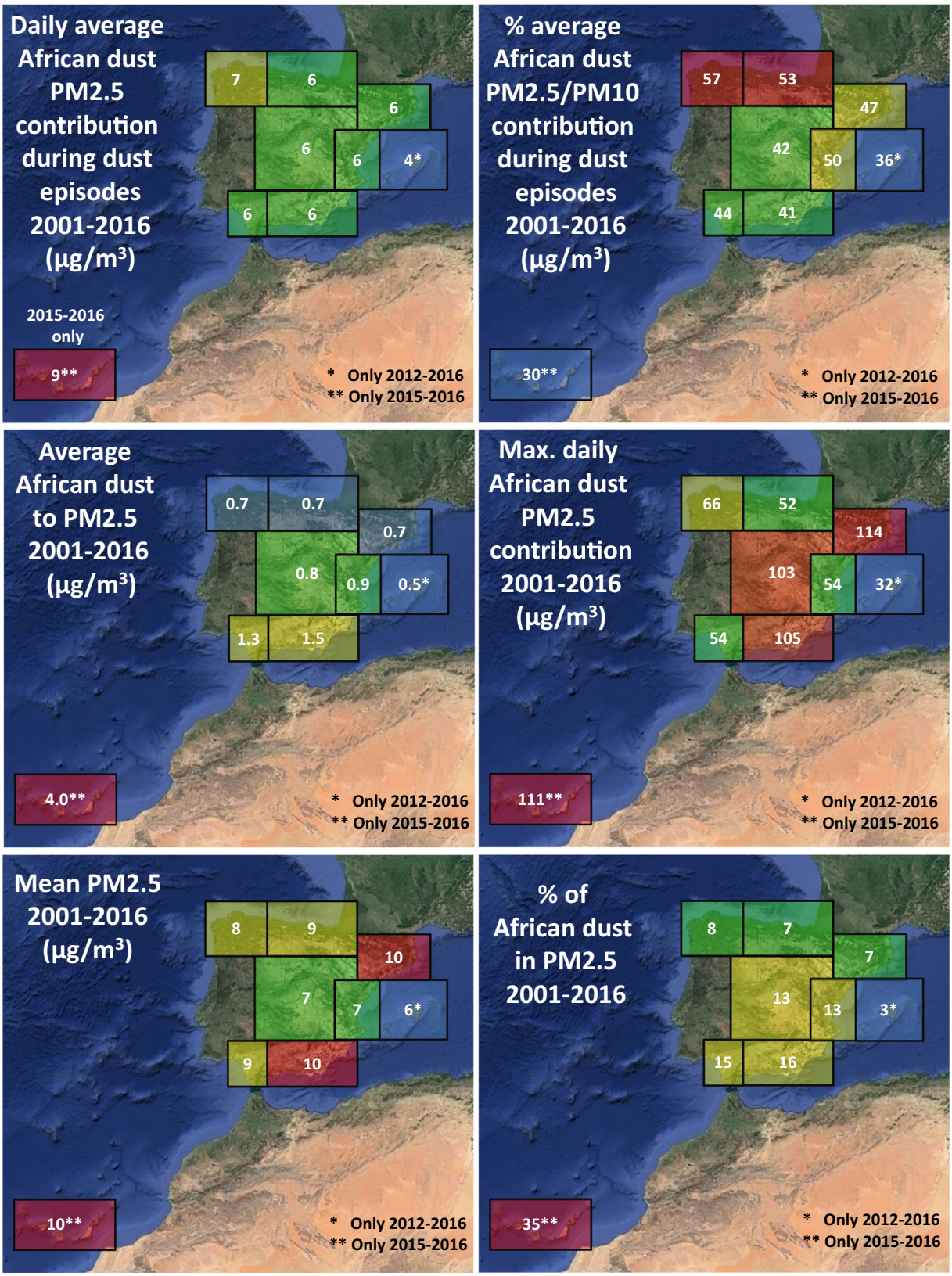

Fig. 3. a) 2001–2016 daily average African dust PM2.5 contribution (µg/m^3) during ADOs for the 9 study regions of Spain. b) Percentage of PM2.5 in PM10 for African dust contribution during ADOs. c) Dust contributions (µg/m^3) to the annual PM2.5 mean. d) Idem for the maxima daily dust contributions to PM2.5 (µg/m^3). e) Average PM2.5 bulk concentrations (µg/m^3). f) Percentage of African dust contributions to the annual PM2.5. Values correspond to averages of annual means of daily levels.

high altitude of the Viznar EMEP air quality monitoring site, located in the Sierra Nevadas at 1265 m a.s.l. This high mountain site is influenced highly by dust transport given that, as reported by Papayannis et al. (2005, 2008), Mona et al. (2006) and Mandija et al. (2017), African dust air masses are preferentially transported at high altitudes over Europe. Also, a gradual increase in the PM2.5/PM10 ratio is evident

(30% in the Canary Islands to 57% in NW Iberia), probably due to both the segregation of finer dust particles as air masses are transported long distances and the larger relative contribution of the local background PMx.

We evaluated also the impact of ADOs on the number of exceedances of the EU daily limit value for PM10 (50 μg/m^3), by selecting the suite with the highest number of such exceedances in each study region. In the Canary Islands the El Rio exceeded this limit value in 8.5% of the days, from which 8.1% were due to ADOs. Viznar station, in the SE region, exceeded the limit value in 3.4% of the days, 3.3% being attributed to ADOs. In the Balearic Islands (Castell de Bellver) these reached 1.7 and 1.6%, respectively; whereas in the SW (Barcarrota), E (Zarra), NE (Els Torms) and Central (Riscollano) Iberia 1.0–1.3 and 0.9–1.2% were reached. In the N region (Niembro) 0.9% of days recorded exceedances of the limit value, but only 0.4% were due to ADOs. Thus as an average, 30 daily exceedances per year are caused by ADOs in the Canary Islands, and 13, 6, 1.5–4 in SE Iberia, Balearic Islands and the rest of Spain, respectively.

3.1.2. Seasonal patterns

As shown in Table 1, 61–70% of all ADO days occur in spring and summer in the different regions of Iberia and in the Balearic Islands, with a higher frequency in summer as we approach Africa and in spring as we approach N and NW Iberia. Thus, most of Iberia (NE, E, SE, SW and Central) records maxima in summer (39–43%), followed by spring (27–32%), with lower frequencies in winter (11–16%) and autumn (15–18%). N Iberia and the Balearic Islands record maxima in summer and spring (31–34% each) and lower percentages in autumn (18–20%) and winter (18% in N Iberia, and, even lower, 13% in the Balearic Islands). In NW Iberia, maxima occur in spring (34%), followed by summer (26%), then winter and autumn (20% each).

In the Canary Islands, ADOs occur all across the year (33, 28 and 25% in winter, summer and autumn, respectively) but with a somewhat lower incidence in spring (14%).

These patterns are aligned with the meteorological scenarios responsible for dust transport towards the Western Mediterranean, as described in Salvador et al. (2014) as a result of a reanalysis study of the period 2001–2011. These authors described four scenarios which explain most dust-transport situations. Among these four situations, the "circulation type I" (characterized by a relative low pressure system observed at the 850 hPa level, W or SW of the Iberian Peninsula coast and by an upper level high located over N Algeria) has a higher impact at the Western than at the Eastern end of the Iberian Peninsula, while "circulation type IV" (characterized by the development of an intense N African high over NEAlgeria and Tunisia) is related to higher impacts in the Central and Eastern areas of Iberia. These two situations occur under weak baric gradient conditions, predominantly in summer but also occurring in other seasons, especially the "circulation type I", which occurs in late spring and early autumn with relatively high frequencies. The "circulation types II and III" (characterized by a shift of the N African high to the west and a trough placed over the Western Iberian Peninsula coast and by a strong high pressure system extended over E Algeria and Libya respectively) are more frequent in spring. In comparison with the other two scenarios, they have associated a stronger baric gradient and a higher impact in NE Iberia and the Balearic Islands.

Table 1
Percent seasonal average occurrence of ADOs over Spain for the period 2001–2016. BAL, Balearic Islands, CAN, Canary Islands.

%	BAL	Iberian Peninsula							CAN
		NW	NE	N	C	E	SE	SW	
WINTER	13	19	11	18	14	13	13	13	33
SPRING	31	34	32	32	28	27	31	31	14
SUMMER	34	26	39	32	43	42	39	39	28
AUTUMN	22	20	18	18	15	18	17	17	25
SUMM SPR	65	61	71	64	70	69	69	69	42
SPRAUT	54	54	50	51	43	45	48	48	39

3.2. ADOs over NE Iberia

3.2.1. Local, regional, continental PMx concentrations

As shown in Table 2, and according to the back-trajectory analysis, the dominant air masses influencing the three monitoring supersites have a NW-W Atlantic origin (NWA, around 30% of the days), followed by the summer regional episodes (25% REG) and winter anticyclonic episodes (15% WAE). The ADO days accounted for 11–15%, this 4% variance might arise either from different data availability at the three sites or air masses from sporadically different origins reaching the CB site, located 175 km from the UB site. This difference may also be related to the preferential transport of dust at higher altitudes over W Europe, as the CB site is situated at 1568 m a.s.l. The proportion of ADO days for these three sites during 2009–2016 is very similar to that obtained for NE Iberia in 2001–2016 (16%).

The back trajectories were computed at 750, 1500 and 2500 m a.g.l. (Section 2.3); however, the altitude of the three sites range from 64 m (Palau Reial) to 1568 m a.s.l. (Montsec). This means that we are actually comparing circulation at different atmospheric levels over the three sites (e.g., 750 m a.g.l. above Palau Reial is about 800 m a.s.l., while at Montsec is about 2250 m a.s.l.). Some biases are probably being introduced due to this mismatch.

The mountain sites are very often influenced by mountain and sea breezes and the diurnal atmospheric convective dynamics, among other meteorological phenomena, that transport pollutants from the valleys towards the top of the mountains, as the regional and continental backgrounds affected by local pollution (Pérez et al., 2008b, 2008c, among others). This transport mechanism gives rise to the typical mountain daily cycles of pollutants with maxima peaking from midday to early afternoon and concentration reductions in the nocturnal periods (Collaud Coen et al., 2013). If we include these midday concentration humps in the calculation of the regional and continental backgrounds levels, then we would overestimate them. Consequently, there is a methodology in widespread use (see GAW protocols from WMO) at mountain sites in order to obtain the actual RB or CB concentration levels of pollution which consists of using concentrations recorded only during the nocturnal period, when the influence of the pollution from surrounding valleys is reduced. However, we should also note that for the circum-Mediterranean basins in the summer conditions, relatively high mountain sites might be permanently included in the ML or be affected by nocturnal reserve polluted strata injected at high altitudes by vertical re-circulations of air masses in a complex orographic and meteorological scenario (Millán et al., 1997, 2000; Millán, 2014; Gangoiti et al., 2001). Bearing these limitations in mind, Table 2 summarises the averaged concentrations for pollutants for different air mass transport scenarios for the RB and CB sites calculated according the concentrations from 19 to 9 h UTC. The average absolute UFP and BC concentrations reached in Barcelona (UB) during ADO days were comparable to those recorded for the other air mass origin, while PM10 concentrations were higher (32 μg/m^3, see Table 2), even when compared with levels recorded during the typical winter anticyclonic episodes (WAEs) with high PM10 (25 μg/m^3). For the finer PM fractions, the European air mass transport (EU) yielded slightly higher PM1 and PM2.5 concentrations than ADOs, but levels during the ADOs were still in the high range when compared to the other air mass transport scenarios and, in both cases, higher than during the typical local WAEs. Levels of PM1–10 and PM2.5–10 during ADO days were 43–46% higher when compared to the average concentrations for non-dust days obtained for the whole period. Very similar patterns, but with lower concentrations, can be deduced for the RB and CB sites (Table 2). For BC, the highest concentrations were obtained at the CB site for ADOs, while for the UB and RB sites, these highest concentrations occur during EU and ASW air mass transport, respectively.

Table 2
2009-2016 frequency of occurrence for the eight air mass transport scenarios, and respective averaged concentrations of UFP (N>10nm), BC, PM10, PM2.5, PM1, PM1-10 and PM1-2.5 measured at the urban, regional and continental background sites (UB, RB, CB). Highest values are underlined. Values correspond to averages of annual means of daily levels.

UB	Days		N>10nm (#/cm^3)		BC (ng/m^3)		PM10 (μg/m^3)		PM2.5 (μg/m^3)		PM1 (μg/m^3)		PM1-10 (μg/m^3)		PM2.5-10 (μg/m^3)		PM1-2.5 (μg/m^3)	
	N	%	Mean	STDV	Mean	STDV	Mean	STDV	Mean	STDV	Mean	STDV	Mean	STDV	Mean	STDV	Mean	STDV
NA	145	6	11251	4147	1299	831	19	7	12	5	9	4	10	5	6	4	4	2
NWA-WA	696	29	12021	4304	1609	1065	22	9	14	7	10	6	12	6	8	4	4	2
SWA	29	1	13077	3500	2644	1510	28	9	20	7	14	7	14	5	9	4	5	2
ADO	270	11	11865	4540	1982	991	32	13	21	8	15	7	17	9	11	6	6	3
MED	74	3	10858	4393	1759	924	26	10	20	8	15	8	11	5	6	3	5	2
EU	172	7	12335	4688	1951	1049	30	13	22	10	17	9	13	6	8	5	5	2
REG	639	27	12030	4335	1557	808	24	8	15	6	11	5	12	5	8	4	4	2
WAE	371	15	11827	4740	1894	1024	25	11	18	8	14	7	12	6	7	4	5	2
Non-ADO	**2396**		**11937**	**4402**	**1669**	**965**	**24**	**9**	**16**	**7**	**12**	**6**	**12**	**5**	**8**	**4**	**4**	**2**

RB	Days		N>10nm (#/cm^3)		BC (ng/m^3)		PM10 (μg/m^3)		PM2.5 (μg/m^3)		PM1 (μg/m^3)		PM1-10 (μg/m^3)		PM2.5-10 (μg/m^3)		PM1-2.5 (μg/m^3)	
	N	%	Mean	STDV	Mean	STDV	Mean	STDV	Mean	STDV	Mean	STDV	Mean	STDV	Mean	STDV	Mean	STDV
NA	150	7	2885	1195	200	153	10	6	8	5	7	4	3	3	2	2	1	1
NWA-WA	692	30	3312	1780	216	192	10	6	8	5	6	4	4	4	2	3	1	1
SWA	34	1	2477	1334	223	235	12	7	9	5	7	5	5	3	2	2	2	2
ADO	270	12	3236	1526	336	207	21	14	13	7	10	5	11	12	8	8	3	5
MED	82	4	1892	1027	304	261	13	7	11	6	9	5	4	3	2	2	1	2
EU	168	7	2920	1569	335	266	15	10	12	8	10	7	5	4	3	3	2	2
REG	544	24	3634	1631	285	176	14	7	10	5	9	4	5	4	4	3	2	2
WAE	367	16	2507	1181	231	228	10	8	8	6	7	6	3	4	2	3	2	2
Non-ADO	**2307**		**3118**	**1534**	**249**	**201**	**12**	**7**	**9**	**5**	**8**	**5**	**4**	**4**	**2**	**4**	**2**	**2**

CB	Days		N>10nm (#/cm^3)		BC (ng/m^3)		PM10 (μg/m^3)		PM2.5 (μg/m^3)		PM1 (μg/m^3)		PM1-10 (μg/m^3)		PM2.5-10 (μg/m^3)		PM1-2.5 (μg/m^3)	
	N	%	Mean	STDV	Mean	STDV	Mean	STDV	Mean	STDV	Mean	STDV	Mean	STDV	Mean	STDV	Mean	STDV
NA	212	13	3057	2217	95	87	6	4	5	3	3	2	3	2	1	2	2	1
NWA-WA	383	24	3263	2397	101	86	7	6	5	4	3	3	3	3	2	2	2	1
SWA	84	5	2435	1525	105	73	5	3	4	3	2	2	3	2	1	1	2	1
ADO	236	15	3158	1792	234	140	20	19	12	10	7	4	13	16	7	10	5	7
MED	34	2	3150	2421	198	159	13	7	10	5	7	4	6	4	3	3	3	1
EU	158	10	3102	1888	202	174	12	8	10	7	8	6	4	4	2	3	2	1
REG	292	18	4220	2133	198	109	15	7	10	6	7	5	7	4	4	3	3	2
WAE	198	12	2890	2469	140	127	9	7	7	6	5	5	3	3	1	2	2	1
Non-ADO	**1597**		**3309**	**2210**	**141**	**108**	**9**	**6**	**7**	**5**	**5**	**4**	**4**	**3**	**2**	**2**	**2**	**1**

BC average concentrations for all measurement days in 2009–2016 reached 1669, 249 and 141 ng/m^3, respectively at the UB, RB and CB sites. Accordingly, and as could be expected the highest levels were recorded at the UB site due to the major, local, primarily-anthropogenic origin of BC in the study area. A similar pattern is observed for UFP, with averaged concentrations of 11,937, 3118 and 3309 #/cm^3, respectively at the UB, RB and CB sites. The much higher levels of UFP at the UB site is also attributed to the major local primary origin of UFP in the area, although nucleation of secondary UFPs may also contribute to increasing the concentrations (Reche et al., 2011; Brines et al., 2015).

The results (Table 2) show clearly that for UFP and BC, levels are much higher for REG and SWA, but also kept high for the other air mass origins, including ADOs. The main differences were detected, as expected, in the very high UB/RB levels of BC for SWA due to the SW transport from a highly trafficked and industrialised area near Barcelona. Higher UFP CB and RB levels were recorded during the REG episodes probably due to high UFP nucleation episodes in this region during the summer (Ripoll et al., 2014; Brines et al., 2015).

As expected, due to the dominant secondary and primary origins of the fine and coarse PM fractions, respectively, the UB/RB/CB ratios are very different for the considered PM size fractions. Average concentrations of PM1, PM2.5 and PM10 in the period 2009–2016 reached 12, 16 and 25 μg/m^3, respectively at the UB; 8, 9 and 12 μg/m^3 at the RB; and 5, 7, and 9 μg/m^3 at the CB (Table 2). These values represent 5, 8 and 12 μg/m^3 PM1 for the CB, RB and UB, respectively, and 4, 4 and 12 μg/m^3 for the coarse fraction (PM1–10).

According to the data from Table 2 the CB average PM1–10 reached 73% of the UB levels for the same PM fraction during ADO days (much higher than the same contribution for the other air mass origins, with an average for non-dust days 34%). Similar relative differences were obtained for these contributions to PM1–2.5. Also for ADOs and PM1, the CB levels reached around 850% of those of the UB ones (similarly to EU and MED origins), while this proportion reached 64% under the REG scenario, 14–36% for the remaining ones. It is interesting to note that these percentages of contributions were relatively maintained for PM2.5 and PM10, with the exception of ADO and REG days. This result points to the higher long- and regional-range transport of PM in summer but also to atmospheric processes favouring the accumulation of local PM1 during ADOs affecting the whole area (Pandolfi et al.,

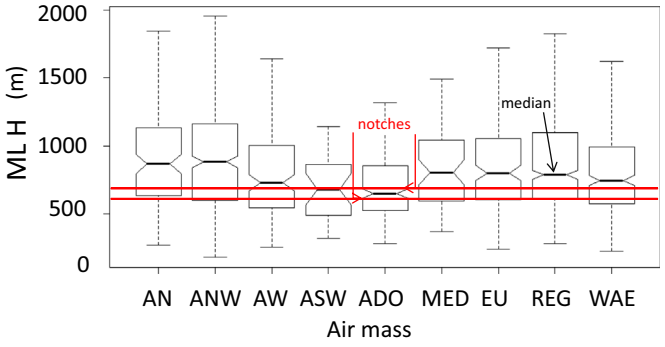

Fig. 4. Boxplots of the 2009–2016 midday MLH measured over Barcelona city for the differentiated air mass transport scenarios. The data are divided into four quartiles. Median is drawn as a horizontal line inside the box. Boxplot notches describe the expected range of variability of the median. If the notches of two boxes do not overlap, this offers evidence of a statistically significant difference between the medians for a 95% confidence interval. The median for ADO days is statistically different from all other medians except the SWA air mass transport.

2014a). The high impact of the ADOs on the levels of locally-emitted pollutants is supported by Fig. 4, which summarises the average MLH, measured at midday in Barcelona, for days with the different air mass transports defined above. The thinest MLH was measured during ADO days (715 ± 272 m), 19% thinner than the average obtained for non-dust days (883 ± 393 m), 23% thinner than the MLH during NWA days (934 ± 417 m), even thinner than during the winter anticyclonic episodes (823 ± 347 m). This thinning of the MLH might contribute to increase levels of regional and local pollutants during ADOs, such as PM1 or other PMx fractions by favouring condensation of local pollutants on dust. In fact, levels of SO_2 and NO_X measured during ADO days were 12 and 6% higher (data not shown here), respectively, when compared with non-dust days. There are also additional factors than might contribute to this increase of levels of anthropogenic pollutants (local and external, gaseous and particulate, fine or coarse) such as: i) the co-transport of pollutants emitted by large industrial states (mostly petrochemical plants) from N Africa, as reported by Moreno et al. (2010), Rodríguez et al. (2011) and Salvador et al. (2016); ii) the transport of pollutants emitted from shipping in the Mediterranean Sea or in the way of the transport to the receptor site (as in the industrial states of Tarragona and those areas to the SW of Barcelona; see evidence below in the section on chemistry); iii) the high dust load during ADOs that might favour the massive condensation of local pollutants on the surfaces of dust particles; and iv) the occurrence of many ADOs in summer, when the capability of the atmosphere to produce secondary PM pollutants is enhanced with respect to the other seasons (in fact average sulphate levels in spring-summer ADOs increase as an average 33% with respect to winter-autumn ADOs, both in PM10 and PM1).

As a whole, it is important to highlight that, as shown in Table 2, ADOs are characterized by the prevalence of the CB load in the averaged levels of the measured PMx, especially in the coarse mode (PM1–10), compared with most of the other air mass origins. It has also to be noted that the differences of altitude of the UB, RB and CB sites might account for a different levels of influence of desert dust being transported preferentially at higher altitudes and this might have introduced biases in our calculations, which cannot be quantified.

3.2.2. PMx speciation

Table 3 summarises the average concentrations of major PM components and trace elements for the three supersites during ADO and non-dust days.

3.2.2.1. Mineral dust. Results of the chemical speciation of PM at the three study supersites in NE Iberia for the period 2009–2016 evidenced that during ADOs, mineral matter (MM, including African dust and regional and local mineral dust, and calculated from the sum of concentrations of bulk Al, Fe, Ti, P and Mn oxides; non-sea salt Na, Mg and K oxides; non sea salt Ca levels, and the indirectly determined Si oxide and carbonate concentration $2.5 * Al_2O_3 = SiO_2$ and, $CO_3^{2-} = 1.5 *$ non-sea salt Ca, Querol et al., 2001) accounted for an average of 10–11 μg/m^3 of PM10 for CB, RB and UB. These concentrations are close to the 13 μg/m^3 2001–2016 averaged dust contribution to PM10 during ADO days obtained for NE Iberia using the statistical method explained in the methodology.

The relative proportions of Al_2O_3, Fe_2O_3 and CaO-mineral (bulkCaO-seasaltCaO, the latter obtained from the Ca/Na ratio of sea salt multiplied by the Na concentrations) reveal differences between the mineral components of dust and their possible origins, with Al_2O_3 indicating a higher content of natural silicate mineral dust ("crustal"), higher CaO being attributed, at least in part, to construction activities (but also local geology and road dust resuspension, Amato et al., 2016), and higher Fe_2O_3 useful as a surrogate for the contributions of non-exhaust vehicle emissions (Amato et al., 2016). When considering all daily data points of PM10 from the UB site, these points have very similar proportions of the three oxides that are independent of the air mass origin, with a slightly higher proportion of Al_2O_3 during ADO days (Fig. 5a). At both the RB and CB sites (Fig. 5b and c), especially at the latest, the proportion of Fe_2O_3 is much less important than it is at the UB site (25–65% at the UB and < 25% at the CB site), except for some specific days (mostly regional) at the RB, when Fe_2O_3 can be higher (sometimes >75%, Fig. 5b), presumably due to the influence of metropolitan Barcelona's urban plume. At the CB site, all days showed similar relative compositions, although ANW days were slightly richer in CaO (Fig. 5c), probably due to the calcareous composition of local soils. For PM2.5, UB samples exhibited a high Fe_2O_3/Al_2O_3 ratio, reflecting the metal content of the traffic-contaminated city air (Fig. 5d). Many of the higher Al_2O_3 relative contents can be traced to the influence of the ADO source, but the highest Al_2O_3 relative values were obtained for regional days (in yellow, Fig. 5d). In general, Fe_2O_3 relative concentrations are higher for PM2.5 than for PM10, especially on ANW and WAE days. In contrast, the lowest proportions of Fe_2O_3 were obtained for the AN air masses. In the case of RB, the PM2.5 diagram is very similar to that for PM10, with higher Fe_2O_3 proportions generally obtained during summer regional pollution episodes (Fig. 5e).

In the case of PM1 (not shown here), with very low MM contributions, a great range of the relative concentrations of the three oxides is evidenced, especially at the UB site. There are no clear trends, although higher Fe_2O_3 contents (>50%) are again more characteristic of the UB than the CB, with a majority of the samples from both the RB and CB sites plotting below $Fe_2O_3 = 25\%$ and scattering between the CaO and Al_2O_3 apices (not shown).

When comparing the geochemical data from the three sites during ADO days (Fig. 6), it becomes apparent again that the UB PM10 composition is richer in Fe_2O_3 (proportionally to the Al and Ca oxides), whereas the RB and CB PM10 samples are similar (with the RB sample being slightly higher in Fe_2O_3 than the CB sample, which is shifted slightly to CaO). It is interesting to note that at both the CB and RB sites, the geochemical data are aligned with the end member, corresponding to the re-suspended soil sampled in the NW Sahara (Moreno et al., 2006), the usual source origin of dust influencing PM levels in Spain (Rodriguez et al., 2001).

Fig. 7a shows the averaged ratios ADO/non-ADO for major PM components in PM10, PM2.5 and PM1 obtained at the UB, RB and CB sites. Results evidence that levels of MM in PM10 increased during ADO days from a factor of 2 (UB) to 4.7 (CB) compared with non-ADO days, very similarly to PM2.5 (2.2 UB to 4.3 RB). In PM1 the increase was less marked (1.1 UB to 2.4 CB) as expected for the coarse size distribution of dust.

3.2.2.2. Organic matter and secondary PM components. For organic matter (OM) (Fig. 7a), there is also a slight increase during ADO days at the UB, RB and CB sites and for the 3 PM fractions, with ADO/non-ADO ratios from 1.1 to 1.4 (UB to CB). In any case, these increases are expected due to OM's seasonality, with a higher summer secondary organic aerosol (SOA) formation rate, when the frequency of ADOs increases (OM/EC ratios increased from the winter-autumn to spring-summer ADOs from 3.9 to 5.5 in PM1 and 4.3 to 5.3 in PM10). Also, a higher summer frequency of sea and mountain breezes that transport pollutants to the mountain sites is recorded compared to other seasons.

Concerning the $nssSO_4^{2-}$ loads, there is also a marked increase during ADO days (Fig. 7a), with ADO/non-ADO ratios from 1.6 to 1.8 in PM10, PM2.5 and PM1 and UB, RB and CB sites. This marked $nssSO_4^{2-}$ increase might be also the result of the marked seasonality of this specie, with higher summer levels, but also to the well-known formation of secondary sulphate on available mineral dust particles (Levin et al., 1996; Alastuey et al., 2005). As stated above at the UB site $nssSO_4^{2-}$ increased 33% in spring-summer ADOs when compared with winter-autumn ADOs. The thinning of the MLH would affect the SOA and SIA in a similar way, but the enrichment in OM is reduced by a factor of 2 compared with the one obtained for the $nssSO_4^{2-}$ loads in PM10 (Table 3). In fact, as shown in Fig. 7b and c, the highest levels of $nssSO_4^{2-}$ are recorded for the ADOs. This increase reaches from 1.6 to 1.8 ADO/non-ADO

Table 3
Averaged concentrations of major PM components and trace elements for the 3 supersites, UB, RB, CB (Urban, Regional and Continental Background) and for ADO and non-ADO days. Values correspond to averages of annual means of daily levels.

	PM10 UB		PM10 RB		PM10 CB		PM2.5 UB		PM2.5 RB		PM1 UB		PM1 RB		PM1 CB	
	ADO	nonados	ADO	nonadoo	ADO	nonados	ADO	nonados	ADO	nonados	ADO	nonados	ADO	nonados	ADO	nonados
N	100	684	98	612	105	621	100	651	82	583	106	699	78	559	58	360
μg/m^3																
PMx	33.4	24.5	25.1	14.5	18.8	8.9	21.0	16.8	15.0	10.3	16.1	12.9	11.8	8.3	7.2	5.4
OM	6.8	6.0	4.8	3.7	4.2	3.1	5.6	5.1	4.1	3.0	4.9	4.3	3.6	2.7	3.9	2.9
EC	1.4	1.2	0.3	0.2	0.2	0.1	1.1	1.0	0.2	0.2	1.0	1.0	0.2	0.2	0.1	0.1
Mineral	10	5.2	9.5	2.4	11	2.4	3.2	1.5	2.3	0.5	0.6	0.5	0.5	0.2	0.9	0.4
nss SO_4^{2-}	4.1	2.3	2.9	1.6	1.8	1.1	3.4	2.0	2.4	1.4	2.6	1.5	2.2	1.3	1.4	1.1
SIA	7.2	5.3	4.5	3.0	3.2	2.2	5.5	4.1	3.4	2.4	4.0	2.9	2.9	1.9	2.2	1.8
Trace elem.	0.2	0.2	0.1	0.1	0.1	0.2	0.1	0.1	0.1	<0.1	0.1	0.1	<0.1	<0.1	<0.1	<0.1
Marine	0.8	0.6	0.4	0.4	0.1	<0.1	0.2	0.2	0.1	0.1	<0.1	<0.1	<0.1	<0.1	<0.1	<0.1
Undet	2.8	3.6	5.6	4.6	<0.1	0.9	1.8	2.7	4.8	4.1	3.0	2.4	4.4	3.2	0.6	0.5
ng/m^3																
Li	0.43	0.23	0.49	0.14	0.61	0.13	0.13	0.09	0.13	0.04	0.04	0.04	0.03	0.01	<0.01	<0.01
Be	0.02	0.01	0.03	<0.01	0.03	<0.01	<0.01	<0.01	0.01	<0.01	<0.01	<0.01	<0.01	<0.01	<0.01	<0.01
P	25	17	19	11	17	7.6	10	8.1	7.1	4.9	5.8	4.7	4.4	3.2	<0.01	<0.01
Sc	0.08	0.04	0.13	0.03	0.12	0.01	0.03	0.01	0.06	0.02	0.04	0.01	0.01	0.01	<0.01	<0.01
Ti	34	17	45	10	56	8.4	10	5.4	11	2.3	2.5	1.8	1.8	0.63	0.25	0.21
V	10	5.4	3.9	1.7	2.8	0.87	8.8	4.3	2.8	1.2	7.0	3.5	2.2	1.1	0.05	0.03
Cr	3.9	3.2	1.6	0.81	1.8	0.77	1.7	1.6	0.81	0.59	0.82	0.79	0.46	0.42	<0.01	<0.01
Mn	12	10	8.8	3.3	10	3.1	5.4	4.6	2.8	1.3	2.0	2.1	1.2	0.53	0.07	0.06
Co	0.28	0.16	0.20	0.07	0.24	0.06	0.14	0.08	0.08	0.03	0.09	0.05	0.05	0.02	<0.01	<0.01
Ni	4.6	2.8	1.8	1.0	1.5	0.64	3.9	2.2	1.4	0.86	3.0	1.8	1.1	0.66	0.08	0.08
Cu	21	20	3.0	2.9	1.7	0.91	6.5	7.1	1.6	1.6	2.8	3.0	1.0	1.1	0.02	0.02
Zn	53	61	12	11	8.0	6.3	37	43	10	9.4	16	19	6.0	5.8	0.07	0.45
Ga	0.18	0.09	0.21	0.05	0.27	0.05	0.07	0.05	0.06	0.02	0.03	0.03	0.01	0.01	<0.01	<0.01
As	0.51	0.41	0.27	0.17	0.26	0.11	0.36	0.31	0.16	0.13	0.28	0.26	0.12	0.11	<0.01	<0.01
Se	0.58	0.39	0.26	0.16	0.16	0.10	0.32	0.29	0.16	0.11	0.16	0.19	0.10	0.09	<0.01	<0.01
Rb	0.83	0.47	0.92	0.29	1.1	0.2	0.28	0.20	0.26	0.10	0.12	0.11	0.10	0.06	<0.01	<0.01
Sr	4.4	2.3	3.4	1.0	4.6	1.2	1.2	0.80	0.91	0.25	0.43	0.28	0.14	0.10	0.05	0.03
Y	0.29	0.19	0.31	0.12	0.53	0.21	0.17	0.12	0.13	0.07	0.11	0.08	0.02	0.04	<0.01	<0.01
Zr	7.9	6.2	6.1	2.8	6.9	3.0	6.1	4.5	5.1	3.4	4.0	3.6	4.2	3.5	<0.01	<0.01
Nb	0.45	0.27	0.50	0.14	0.62	0.10	0.18	0.11	0.20	0.07	0.09	0.07	0.07	0.05	<0.01	<0.01
Mo	2.8	3.6	1.5	1.3	0.70	0.79	4.2	2.5	0.39	1.30	2.8	1.8	<0.01	0.86	<0.01	<0.01
Cd	0.14	0.15	0.06	0.05	0.04	0.02	0.14	0.12	0.06	0.05	0.07	0.08	0.04	0.04	<0.01	<0.01
Sn	5.2	4.9	0.77	0.64	0.33	0.27	2.7	2.4	0.57	0.46	1.8	1.5	0.44	0.40	<0.01	<0.01
Sb	2.5	2.3	0.33	0.27	0.13	0.07	1.0	0.8	0.20	0.16	0.54	0.39	0.16	0.13	<0.01	<0.01
Cs	0.05	0.03	0.05	0.01	0.06	0.01	0.01	0.01	0.01	<0.1	0.00	0.00	0.00	0.00	<0.01	<0.01
Ba	16	12	7.2	3.2	7.7	2.4	8.4	8.0	2.8	2.2	2.9	3.4	0.38	0.86	0.10	0.07
La	0.42	0.21	0.44	0.12	0.61	0.13	0.16	0.09	0.13	0.05	0.06	0.05	0.03	0.02	<0.01	<0.01
Ce	0.82	0.42	0.90	0.23	1.2	0.25	0.31	0.19	0.27	0.08	0.14	0.12	0.06	0.05	<0.01	<0.01
Pr	0.08	0.04	0.10	0.02	0.14	0.03	0.02	0.01	0.03	0.01	0.01	0.01	0.01	<0.01	<0.01	<0.01
Nd	0.28	0.12	0.37	0.09	0.52	0.12	0.09	0.05	0.11	0.03	0.03	0.02	0.02	0.01	<0.01	<0.01
Sm	0.06	0.03	0.08	0.02	0.12	0.04	0.02	0.02	0.02	0.01	0.01	0.01	<0.01	<0.01	<0.01	<0.01
Eu	0.01	<0.01	0.01	<0.01	0.02	0.01	<0.1	<0.01	<0.01	<0.01	0.00	<0.01	<0.01	<0.01	<0.01	<0.01
Gd	0.07	0.04	0.08	0.02	0.12	0.05	0.03	0.02	0.03	0.01	0.02	0.01	0.01	0.01	<0.01	<0.01
Tb	0.02	0.01	0.01	<0.01	0.02	0.01	0.01	0.01	0.01	<0.01	0.00	<0.01	<0.01	<0.01	<0.01	<0.01
Dy	0.06	0.04	0.07	0.03	0.12	0.06	0.04	0.03	0.03	0.02	0.03	0.02	0.01	0.01	<0.01	<0.01
Ho	0.01	0.01	0.01	0.01	0.02	0.01	0.01	0.01	0.01	<0.01	0.00	<0.01	<0.01	<0.01	<0.01	<0.01
Er	0.03	0.02	0.03	0.01	0.06	0.02	0.01	0.01	0.01	0.01	0.01	0.01	<0.01	<0.01	<0.01	<0.01
Tm	<0.01	<0.01	<0.01	<0.01	<0.01	<0.01	0.00	0.00	<0.01	<0.01	0.00	<0.01	<0.01	<0.01	<0.01	<0.01
Yb	0.01	<0.01	0.03	0.01	0.05	0.02	0.00	0.00	0.01	0.01	0.00	<0.01	<0.01	<0.01	<0.01	<0.01
Lu	0.02	0.01	<0.01	<0.01	<0.01	<0.01	0.01	0.01	<0.01	<0.01	0.01	<0.01	<0.01	<0.01	<0.01	<0.01
Hf	0.29	0.24	0.23	0.09	0.22	0.08	0.23	0.17	0.19	0.12	0.15	0.13	0.17	0.13	<0.01	<0.01
Tl	0.04	0.05	0.01	<0.01	0.01	<0.01	0.03	0.03	<0.01	<0.01	0.02	0.02	<0.01	<0.01	<0.01	<0.01
Pb	8.0	7.9	3.0	2.1	2.1	0.93	6.1	5.9	2.5	1.8	3.6	3.7	1.9	1.4	0.13	0.07
Bi	0.34	0.37	0.10	0.11	0.03	0.02	0.17	0.20	0.06	0.07	0.10	0.12	0.05	0.05	<0.01	<0.01
Th	0.14	0.07	0.16	0.04	0.19	0.05	0.06	0.03	0.06	0.02	0.03	0.02	0.01	0.01	<0.01	<0.01
U	0.11	0.08	0.08	0.06	0.16	0.11	0.08	0.06	0.06	0.05	0.05	0.05	0.03	0.04	<0.01	<0.01

concentrations and 2.3 to 3.0 for ADO/NA days for PM10 (Fig. 7b), and 1.3–1.7 and 2.4–2.7, respectively for PM1 (Fig. 7c). For OM (Fig. 7d and e, these enrichments are much reduced during ADOs (ratios 1.1 to 1.4) and similar or lower than those obtained for the EU and WAE atmospheric scenarios. If we consider SIA ($ssSO_4^{2-}$ $NH_4NO_3^-$), the ADO enrichments are intermediate between those of $nssSO_4^{2-}$ and OM. The higher enrichment of $nssSO_4^{2-}$ compared to SIA and SOA (major component of OM) points to a relevant dust-SO_4^{2-} chemical interaction.

3.2.2.3. Trace PM components. Concerning trace elements (Table 3), the contents of typical crustal elements, such as Be, Ga, Hf, Li, Mn, P, Rb, Th, Ti, U, Y, Zr and Rare Earth Elements (REEs) were markedly higher during ADO days, compared to the rest of the air mass origins, while those of Cr, Cu, Zn, Ge, As, Sn, Sb, W, Tl and Pb were higher during SWA transport days. Many of the latter are associated mostly with metallurgical industrial sources located to the SW of Barcelona (Mn, Ni, As, Cd, Bi, Cr, Cu, Zn, Sn, Sb, W, Pb), shipping (V and Ni) or non-exhaust vehicle emissions (Ba, Zn, Cu, Sn, Sb, Mn), according to latest published

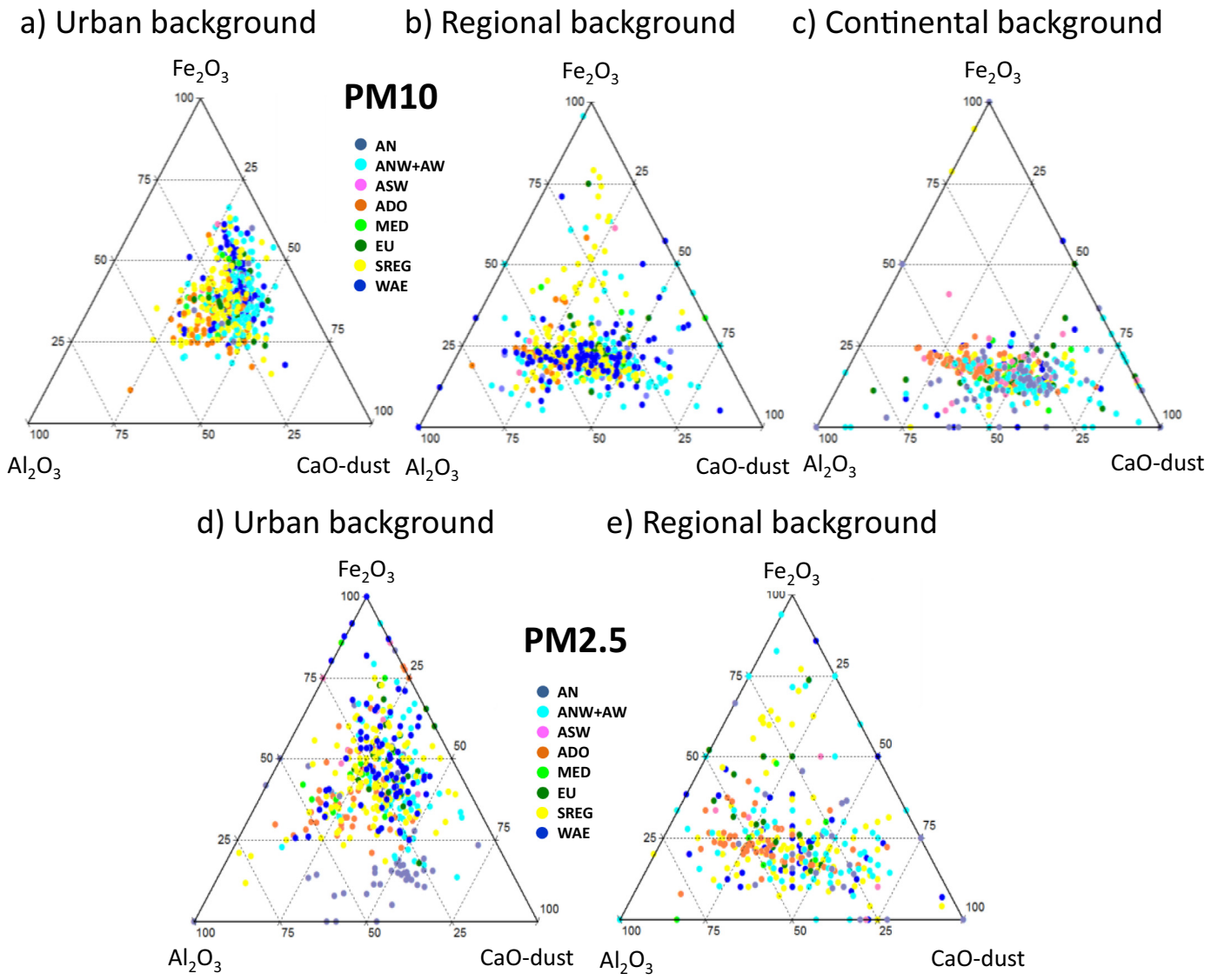

Fig. 5. Al_2O_3-Fe_2O_3 and CaO ternary diagram for PM10 samples for all days as measured for the urban (a), regional (b) and continental (c) background sites. Idem for PM2.5 for the urban (d) and regional (e) background sites.

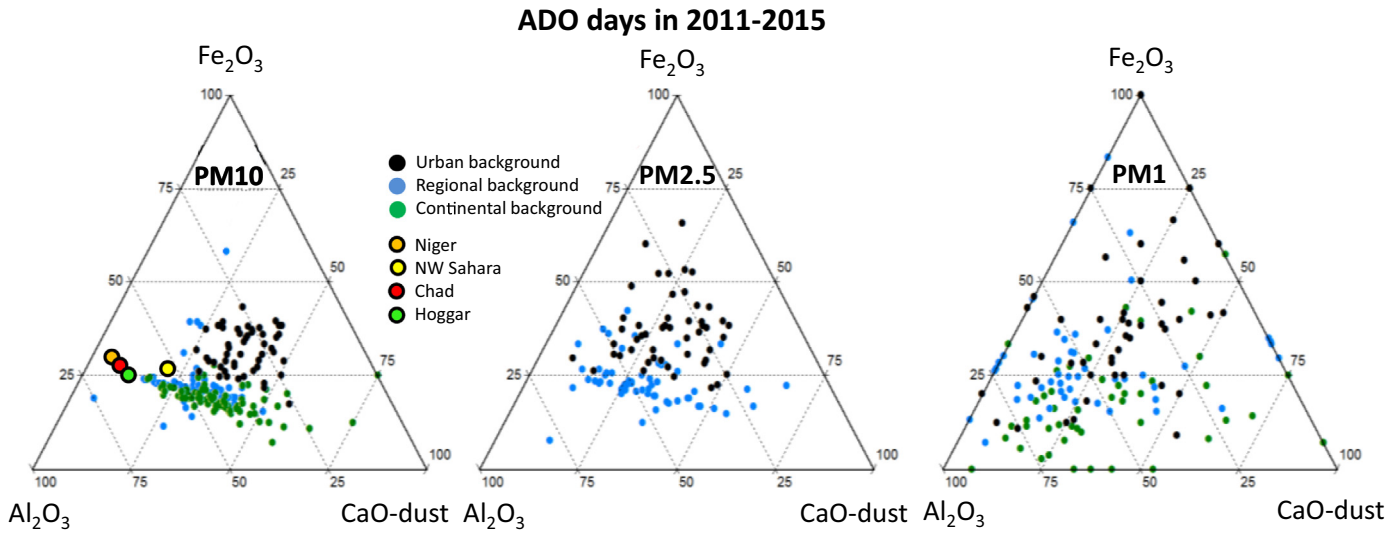

Fig. 6. Al_2O_3-Fe_2O_3 and CaO ternary diagram for PM10, PM2.5 and PM1 samples as measured, for ADO days at the urban, regional and continental background sites, as well as the resuspended particles from soils from Niger, NW Sahara, Chad and Hoggar Basin (all in N Africa), as reported by Moreno et al. (2006).

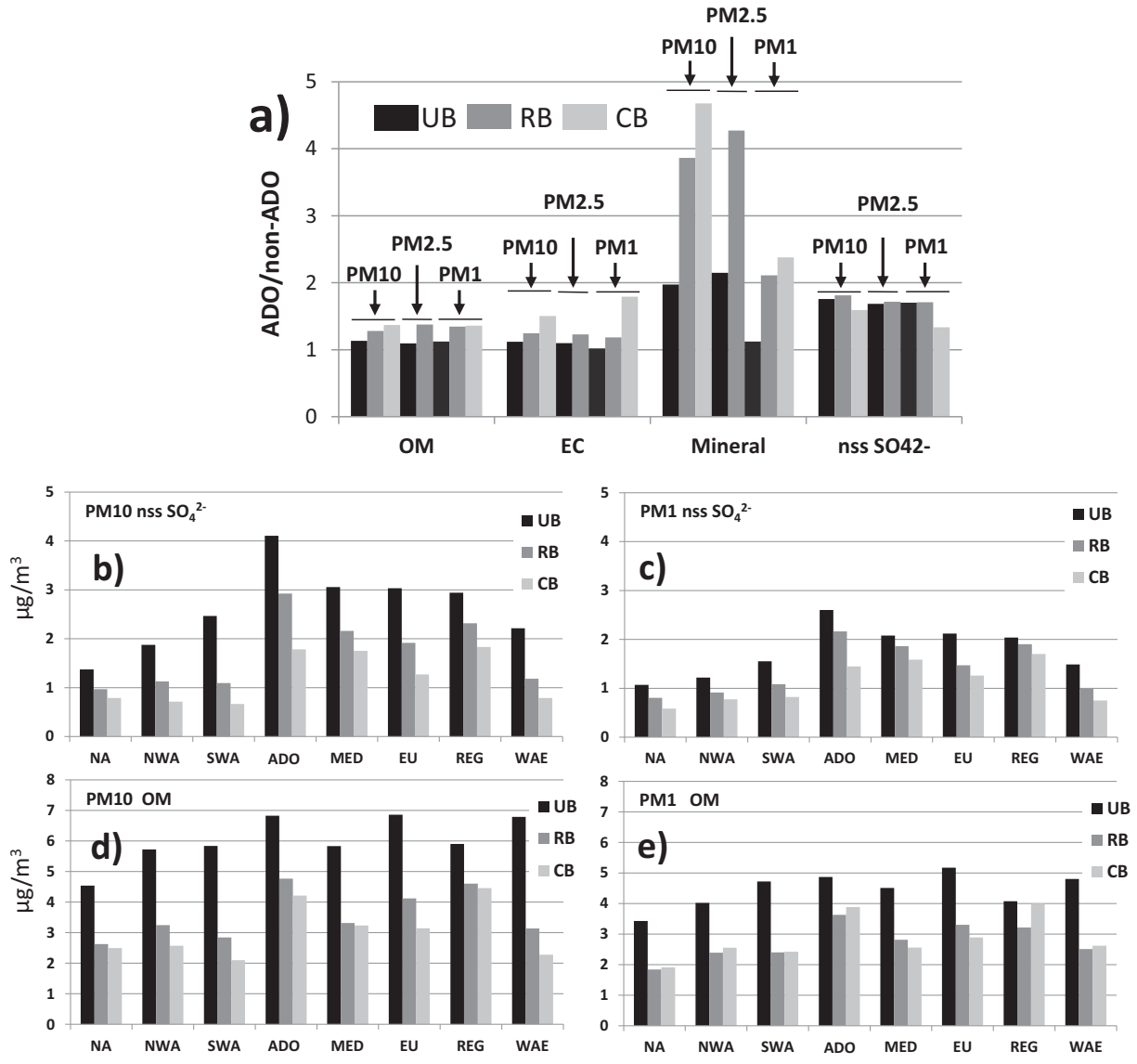

Fig. 7. a) Ratios for ADO/nonADO average concentrations at the UB, RB, and CB sites for organic matter (OM), non-sea salt sulphate ($nssSO_4^{2-}$) and mineral mater (Mineral) in PM10, PM2.5 and PM1; and averaged levels of $nssSO_4^{2-}$ (b) in PM10 and c) in PM1 and OM (d) in PM10 and e) in PM1 for the different air mass transport scenarios identified in this study. UB, RB, CB stand for urban, regional and continental background levels.

source apportionment analysis carried out for PM in Barcelona (Amato et al., 2009, 2016).

The UB/RB ratio of the concentrations of trace elements in PM10 during ADOs supports the discrimination of those elements being transported with African dust (UB/RB ratio close to 1) from those accumulated locally during the ADO. Accordingly, the following groups have been differentiated (Fig. 8):

- Elements with an African dust origin, i.e., with a UB/RB ratio < 1.5: Li, Be, P, Sc, Ti, Ga, Rb, Sr, Y, Zr, Nb, Cs, REEs, Hf, Th and U.
- Elements enriched locally during the ADO, i.e., with a UB/RB ratio =

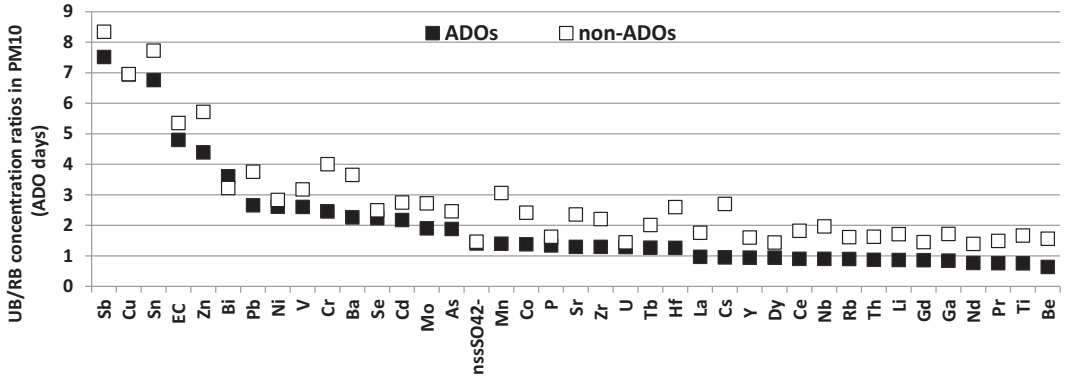

Fig. 8. Urban/regional background ratio (UB/RB) of averaged trace elements concentrations measured in PM10 during African dust outbreaks.

1.5–3: V, Cr, Co, Ni, As, Se, Mn, Mo, Cd, Ba and Pb; or a UB/RB ratio > 3: Cu, Zn, Sn, Sb, Tl and Bi.

For non-ADO days (Fig. 8) these groups are still differentiated but the local enrichment is higher probably because the lower RB levels of most elements during non-ADO dats.

Moreover, when evaluating concentrations in μg/g, i.e., by dividing the trace element concentrations (μg/m^3) by PM10 mass concentrations (g/m^3), it becomes evident that at the UB site, the same groups of elements are differentiated with respect to the enrichment in PM10 during ADOs compared with non-ADOs days:

- Elements highly enriched in PM10 during ADOs and mainly associated with African dust: Sc, Ti, Be and REEs >50%; Li, Ge, V, Ga, Rb, Sr, Y and Co 25 to 50%.
- Elements moderately enriched or not enriched and thus partially associated with African dust: Ni, Se, Nb, P, Ba and Zr at −5 to 20%.
- Elements highly or slightly depleted in PM10 during ADOs and thus with a local origin because African mineral dust dilutes their concentrations in PM10, in spite of their possible concentration increments due to the thinning of the ML: As, Mn, Cr, Sb, Sn, Cu, Pb, Cd, Bi. Zn, Tl and Mo at −8 to −42%.

When the same exercise is done for the PM10 at the RB and CB sites, the same elemental classification is obtained but with higher relative enrichments and reduced depletions.

Titanium has been identified as one of the best tracers of the ADOs in the urban atmosphere of Barcelona (Querol et al., 2001). To evaluate quantitatively the magnitude of the effect of the ADO enrichment of locally and regionally emitted pollutants, compared with that of non-ADO days, we carried out calculations of Ti-normalised Enrichment Factors (EFs) for the major and trace PM10 components analysed here by following the Eqs. (1) and (2).

$$EF_{PM10\_iUB/RB} = \frac{\frac{PM10\_UB_i}{PM10\_UB_{Ti}}}{\frac{PM10\_RB_i}{PM10\_RB_{Ti}}} \quad (1)$$

$$EF_{PM10\_iUB/CB} = \frac{\frac{PM10\_UB_i}{PM10\_UB_{Ti}}}{\frac{PM10\_CB_i}{PM10\_CB_{Ti}}} \quad (2)$$

Here, $EF_{PM10\_iUB/RB}$ and $EF_{PM10\_iUB/CB}$ are the Ti-normalised EFs of the PM10 component 'i' in the UB divided by that of the RB or CB, respectively; $PM10\_UB_i$, $PM10\_RB_i$ and $PM10\_CB_i$ and $PM10\_UB_{Ti}$, $PM10\_RB_{Ti}$ and $PM10\_CB_{Ti}$ are the averaged ambient air concentrations of PM10 components 'i' and Ti at the UB, RB and CB sites. These EFs were calculated for both ADO and non-ADO days (ADO-$EF_{PM10\_iUB/RB}$ and ADO-$EF_{PM10\_iUB/CB}$ and Non-ADO-$EF_{PM10\_iUB/RB}$ and Non-ADO-$EF_{PM10\_iUB/CB}$ (Fig. 9), and the following groups of PM10 components were identified based on their respective EF values:

- Be, Cs, Ga, Hf, Li, mineral matter Sr, Rb, Th, U, Y, Zr and REEs reached $EF_{iUB/RB}$ and $EF_{iUB/CB}$ from 0.8 to 1.7, thus evidencing a null to light enrichment in the UB compared to the RB 'i'/Ti concentrations. Also, the EFs for most of them were very similar for ADO and non-ADO days (ADO-EF/Non-ADO-EF = 0.8–1.5 for most elements). Thus, nss-SO_4^{2-} was enriched by around 60% in the UB during ADO days, nearly double that of the non-ADO days. In addition to the possible long-range transport (see below) and the accumulation of this pollutant due to the MLH thinning, the interaction of local and regional SO_2 and H_2SO_4 with mineral dust particles has been identified as a main cause of its enrichment in ADOs.
- Typical road traffic-related PM components, such as Sb, Cu, Sn, EC, Zn and Bi, reached extremely high EFUB/RBs (10.0–4.8) and EFUB/CBs (31.0–11.0) during ADOs, and the EFs where 1.7 to 2.9 higher in

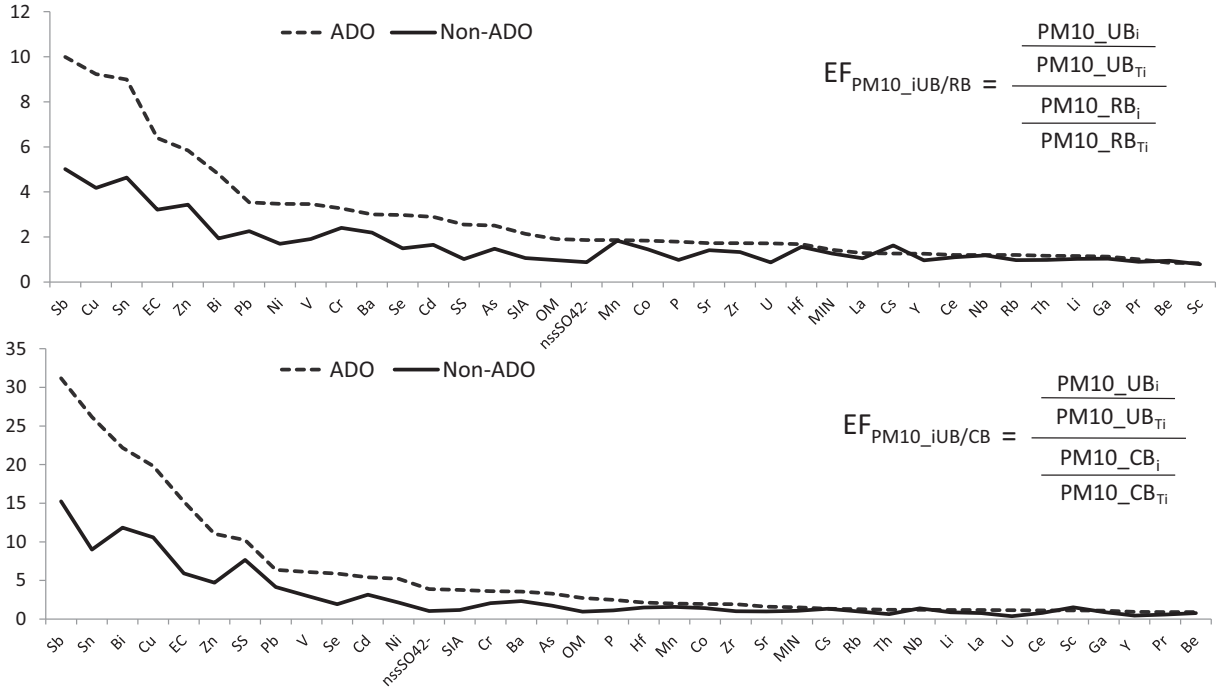

Fig. 9. Ratios of UB/RB (upper) and UB/CB (lower) Ti-normalised Enrichment Factors (EF) values for major and trace PM10 components for African dust outbreaks (ADO) and non-ADO days.

ADOs than non-ADOs. Thus, as could be expected, the road traffic-related PM components are highly enriched vs Ti at the UB site, but this enrichment is more than doubled in ADO days compared with non-ADO days.

- Intermediate EFs (1.6 to 3.2 for EFUB/RB and 1.8–7.7 for EFUB/CB during ADOs) were obtained for Pb, Ni, V, Cr, Ba, Se, Cd, SS, As, SIA, OM, nssSO_4^{2-}, Mn, Co, P and sea salt, which arise in large proportions from regional emissions from industry (Pb, Cr, Cd, Co, Ni, As, Se, Mn) and shipping (V and Ni), according the latest source apportionment analyses (Amato et al., 2016). Furthermore, for most of these PM components (Pb, Cd, Ni, V, sea salt, As, Se, SIA and OM), the EFs in ADO days were doubled (1.0–3.8) compared with non-ADO days. Thus, for these, mainly regional, pollutants, there was a moderate enrichment during ADO days, but, in any case, this enrichment wad double the one calculated for non-ADO days. For some of these components and the ones from the first group, the co-transport with dust of anthropogenic pollutants emitted by large industrial states (mostly petrochemical plants) in N Africa and the Mediterranean-wide shipping emissions (Moreno et al., 2010; Rodríguez et al., 2011) might also account for their moderate EFs during ADOs. Non-sea salt-SO_4^{2-} at the UB site was enriched by a factor ranging from 1.3 (versus summer regional episodes) to 3.0 (versus N Atlantic air mass transport) during ADO days and nearly double that of the non-ADO days. In addition to the possible long-range transport (see below) and the accumulation of this pollutant due to the MLH thinning, the above referred interaction of local and regional SO_2 and H_2SO_4 with mineral dust particles has been identified as a main cause of its enrichment in ADOs.

The above results on EFs suggest that ADOs favour the accumulation of, or co-exist with, locally and/or regionally emitted PM components; hence, mineral dust is not the only pollutant affecting air quality during African dust episodes. Since it would be expected reduction of the MLH to affect the both primary and secondary PM components in a similar proportion, our results indicate the enhancement is larger for primary local species in the coarse fraction.

4. Conclusions

This study focuses on the assessment, based on a multi-parametric dataset, of air quality degradation over Spain induced by African Dust Outbreaks (ADOs). To this end, we evaluated the 2001–2016 occurrences of ADOs over Spain and their associated impact on the levels of PM10 and PM2.5. Furthermore, for NE Iberia, we analysed in detail the impact of ADOs on other metrics, including UFP, BC and the levels and compositions of PM1, PM2.5, PM10, by comparing the 8-year records obtained simultaneously at three (urban, regional, and continental background) sites, in and around Barcelona City.

Results show a clear decrease of dust in PM10 and PM2.5 as the distance to N Africa increases, from the maxima of the Canary Islands and SE Iberia (33–35% of annual averaged PM10 and PM2.5 from regional background sites are attributed to ADOs) to the minimum at N Iberia (7–10%). A marked seasonality of ADOs is observed, with 67–77% of all ADO days occurring in spring and summer in most regions of Iberia and in the Balearic Islands, but this pattern contrasts to their prevalence in autumn and spring in NW Iberia (76%) and their distribution throughout the year in the Canary Islands, although there are fewer episodes in spring (13%) there.

Focusing on NE Iberia, the average UFP and BC concentrations measured in the Barcelona urban background during ADO days were comparable to those recorded for the other air mass origins, while mean levels of PM10 were even higher than those measured during the typical "urban pollution events" occurring in winter under stagnant anticyclonic scenarios. For the finer PM fractions, PM1 and PM2.5 concentrations during ADOs were slightly lower than those observed during EU air mass transport, but still ranked highly compared to all air mass transport scenarios. Levels of PM1–10 in the Barcelona City during ADO days were 43–46% higher compared to non-dust days. In the regional and continental background this increase reached 175 and 225%.

When comparing levels of pollutants in the urban background of Barcelona City, and the surrounding regional and continental backgrounds for ADOs and non-ADOs days we found that UFP and BC do not markedly increases during ADO days. However, PM1–10 and PM1–2.5 levels in the continental background site during ADO days reached 70–75% of the equivalent ones measured at the urban background, whereas this reaches 34% for non-ADO days.

The study of the variation in the relative contributions of Al_2O_3, Fe_2O_3 and CaO to the dust fraction evidenced that Al_2O_3 can be considered a good tracer of African dust. Concentrations of CaO at the urban site are clearly affected by the resuspension of local soils, construction activities and road dust, whereas concentrations of Fe_2O_3 are clearly affected by anthropogenic emissions, mainly brake discs from vehicles. This confirms the limitation of using CaO and Fe_2O_3 as tracers of African dust, as concluded by Alastuey et al. (2016) for specific episodes.

Both continuous measurements of PMx levels and chemical speciation allowed us to evidence that the increased concentrations during ADOs are caused by the following factors:

- The transport of mineral matter from desert dust, frequently causing exceedances of the daily PM10 standards when added to the local and regional PM, as demonstrated in this study and a number of prior ones (Rodriguez et al., 2001; Querol et al., 2009; Pey et al., 2013; among others).
- The co-transport of dust with anthropogenic pollutants emitted by large petrochemical plants from N Africa and Mediterranean-wide shipping emissions. Levels of nssSO_4^{2-}, V and Ni that were closely related to these sources were found to be high during ADOs. Moreno et al. (2010) and Rodríguez et al. (2011) also evidenced this co-transport.
- The accumulation of locally-emitted anthropogenic PM pollutants (SO_4^{2-}, As, Bi, Cu, Cd, EC, Pb, Sn, Sb, among others) during ADOs, which has been evidenced in our study using Ti-normalised enrichment factors. This accumulation can be attributed to:
  - o A relatively low MLH (even thinner than during WAEs, around 20% thinner at midday than the average obtained for non-ADO days in our study).
  - o The high dust load during ADOs favouring the formation of secondary pollutants from local semi-volatile chemicals on the surface of mineral particles. This scenario is especially plausible in the case of nssSO_4^{2-}.
  - o ADO frequency in most of mainland Spain is higher in summer, when the capability of the atmosphere to produce secondary PM pollutants is larger than during the other seasons.

In view of the above results, we would like to highlight that patterns of PM during ADOs are very complex and this might influence human health. As a consequence, not only the measure of PMx levels has to be quantitatively contrasted with potential health effects. The occurrence of ADOs also favours the occurrence of individual or synergistic effects that might involve meteorology, the preferential accumulation of locally-emitted pollutants and the long-range co-transport of anthropogenic pollutants, giving rise to increases in the levels of secondary PM species and metals in metropolitan areas, such as Barcelona, with high population densities. The impact of this complex mix of PM compounds on human health should be also assessed in health assessment analyses of ADOs. Thus, it is not only mineral dust that matters in terms of air quality during African dust episodes.

Acknowledgements

This study was supported by the Spanish Ministry for the Ecological Transition with a number of research contracts to investigate air quality problems in Spain, the Spanish Ministry of Science, Innovation and Universities and FEDER funds under the project HOUSE (CGL2016-78594-R), the ACTRIS2 project (grant agreement No. 654109) financed by the European Union's Horizon 2020 - Research and Innovation Framework Programme, the Department of Territory and Sustainability and the Catalan Research Agency (AGAUR 2017 SGR41) of the Generalitat de Catalunya. The authors gratefully acknowledge the NOAA Air Resources Laboratory (ARL) for the provision of the HYSPLIT transport and dispersion model (http://www.ready.noaa.gov); and to BSC, Barcelona Supercomputing Centre (https://ess.bsc.es/bsc-dust-daily-forecast), SKIRON-Simulations from the University of Athens (http://forecast.uoa.gr/dustindx.php), and the NAAPs-Navy Research Laboratory outputs (https://www.nrlmry.navy.mil/aerosol_web/) for the open access to their dust forecast systems. The authors wish to thank the Catalan Meteorological Service for providing the BCN radio-sounding data. Marco Pandolfi is funded by a Ramón y Cajal Fellowship (RYC-2013-14036) awarded by the Spanish Ministry of Science, Innovation and Universities.

Appendix A. Supplementary data

Supplementary data to this article can be found online at https://doi.org/10.1016/j.scitotenv.2019.05.349.

References

Achilleos, S., Evans, J.S., Yiallouros, P.K., Kleanthous, S., Schwartz, J., Koutrakis, P., 2014. PM10 concentration levels at an urban and background site in Cyprus: the impact of urban sources and dust storms. J. Air Waste Manage. Assoc. 64, 1352–1360.

Alastuey, A., Querol, X., Castillo, X., Avila, A., Cuevas, E., Estarellas, C., Torres, C., Exposito, F., García, O., Diaz, J.P., Van Dingenen, R., Putaud, J.P., 2005. Characterisation of TSP and PM2.5 at Izaña and Sta. Cruz de Tenerife (Canary Islands, Spain) during a Saharan dust episode (July 2002). Atmos. Environ. 39, 4715–4728.

Alastuey, A., Querol, X., Aas, W., Lucarelli, F., Pérez, N., Moreno, T., Cavalli, F., Areskoug, H., Balan, V., Catrambone, M., Ceburnis, D., Cerro, J.C., Conil, S., Gevorgyan, L., Hueglin, C., Imre, K., Jaffrezo, J.-L., Leeson, S.R., Mihalopoulos, N., Mitosinkova, M., O'Dowd, C.D., Pey, J., Putaud, J.-P., Riffault, V., Ripoll, A., Sciare, J., Sellegri, K., Spindler, G., Yttri, K.E., 2016. Geochemistry of PM10 over Europe during the EMEP intensive measurement periods in summer 2012 and winter 2013. Atmos. Chem. Phys. 16 (10), 6107–6129.

Amato, F., Pandolfi, M., Escrig, A., Querol, X., Alastuey, A., Pey, J., Perez, N., Hopke, P.K., 2009. Quantifying road dust resuspension in urban environment by multilinear engine: a comparison with PMF2. Atmos. Environ. 43, 2770–2780.

Amato, F., Alastuey, A., Karanasiou, A., Lucarelli, F., Nava, S., Calzolai, G., Severi, M., Becagli, S., Gianelle, V.L., Colombi, C., Alves, C., Custódio, D., Nunes, T., Cerqueira, M., Pio, C., Eleftheriadis, K., Diapouli, E., Reche, C., Minguillón, M.C., Manousakas, M.I., Maggos, T., Vratolis, S., Harrison, R.M., Querol, X., 2016. AIRUSE-LIFE: a harmonized PM speciation and source apportionment in five southern European cities. Atmos. Chem. Phys. 16, 3289–3309.

Bergametti, G., Dutot, A.L., Buat-Menard, P., Losno, R., Remoudaki, E., 1989a. Seasonal variability of the elemental composition of atmospheric aerosolparticl es over the NW Mediterranean. Tellus 41B, 353–361.

Bergametti, G., Gomes, L., Coude-Gaussen, G., Rognon, P., Le Coustumer, M.N., 1989b. African dust observed over Canary Islands: source regions identification and transport pattern for some summer situation. Journalof Geophysical Research 94, 14855–14864.

Brines, M., Dall'osto, M., Beddows, D.C.S., Harrison, R.M., Gómez-Moreno, F., Núñez, L., Artíñano, B., Costabile, F., Gobbi, G.P., Salimi, F., Morawska, L., Sioutas, C., Querol, X., 2015. Traffic and nucleation events as main sources of ultrafine particles in high insolation developed world cities. Atmos. Chem. Phys. 15, 5929–5945.

Collaud Coen, M., Andrews, E., Asmi, A., Baltensperger, U., Bukowiecki, N., Day, D., Fiebig, M., Fjaeraa, A.M., Flentje, H., Hyvärinen, A., Jefferson, A., Jennings, S.G., Kouvarakis, G., Lihavainen, H., Lund Myhre, C., Malm, W.C., Mihapopoulos, N., Molenar, J.V., O'Dowd, C., Ogren, J.A., Schichtel, B.A., Sheridan, P., Virkkula, A., Weingartner, E., Weller, R., Laj, P., 2013. Aerosol decadal trends – part 1: in-situ optical measurements at GAW and IMPROVE stations. Atmos. Chem. Phys. 13, 869–894. https://doi.org/10.5194/acp-13-869-2013.

Dayan, U., Heffter, J., Miller, J., Gutman, G., 1991. Dust intrusion events into the Mediterranean basin. J. Appl. Meteorol. 30, 1185–1199.

Díaz, J., Tobías, A., Linares, C., 2012. Saharan dust and association between particulate matter and case-specific mortality: a case-crossover analysis in Madrid (Spain). Environ. Health 11 (1), 11. http://ehjournal.biomedcentral.com/articles/10.1186/1476-069X-11-11.

Díaz, J., Linares, C., Carmona, R., Russo, A., Ortiz, C., Salvador, P., Machado Trigo, R., 2017. Saharan dust intrusions in Spain: health impacts and associated synoptic conditions. Environ. Res. 156, 455–467.

Ealo, M., Alastuey, A., Pérez, N., Ripoll, A., Querol, X., Pandolfi, M., 2018. Impact of aerosol particle sources on optical properties in urban, regional and remote areas in the North-Western Mediterranean. Atmos. Chem. Phys. 18, 1149–1169. https://doi.org/10.5194/acp-18-1149-2018.

EC, 2011. Commission Staff Working Paper Establishing Guidelines for Determination of Contributions From the Re-suspension of Particulates Following Winter Sanding or Salting of Roads Under the Directive 2008/50/EC on Ambient Air Quality and Cleaner Air for Europe. vol. 207. European Commission, SEC 2011. 43 pp. http://ec.europa.eu/environment/air/quality/legislation/pdf/sec_2011_0207.pdf.

Escudero, M., Castillo, S., Querol, X., Avila, A., Alarcón, M., Viana, M.M., Alastuey, A., Cuevas, E., Rodríguez, S., 2005. Wet and dry African dust episodes over Eastern Spain. J. Geophys. Res. 110, D18S08 (10.1029).

Escudero, M., Querol, X., Ávila, A., Cuevas, E., 2007a. Origin of the exceedances of theEuropean daily PM limit value in regional background areas of Spain. Atmos. Environ. 41, 730–744.

Escudero, M., Querol, X., Pey, J., Alastuey, A., Pérez, N., Ferreira, F., Cuevas, E., Rodríguez, S., Alonso, S., 2007b. A methodology for the quantification of the net African dust load in air quality monitoring networks. Atmos. Environ. 41, 5516–5524.

Gangoiti, G., Millán, M.M., Salvador, R., Mantilla, E., 2001. Long-range transport and re-circulation of pollutants in the western Mediterranean during the project Regional Cycles of Air Pollution in the West-Central Mediterranean Area. Atmos. Environ. 35, 6267–6276. https://doi.org/10.1016/S1352-2310(01)00440-X.

Ginoux, P., Garbuzov, D., Hsu, H.C., 2010. Identification of anthropogenic and natural dust sources using Moderate Resolution Imaging Spectroradiometer (MODIS) Deep Blue level 2 data. J. Geophys. Res. 115, D05204. https://doi.org/10.1029/2009JD012398.

Ginoux, P., Prospero, J.M., Gill, T.E., Hsu, N.C., Zhao, M., 2012. Global-scale attribution of anthropogenic and natural dust sources and their emission rates based on MODIS Deep Blue aerosol products. Rev. Geophys. 50, RG3005. https://doi.org/10.1029/2012RG000388.

Holzworth, C.G., 1964. Estimates of mean maximum mixing depths in the contiguous United States. Mon. Weather Rev. 92, 235–242.

Huneeus, N., Schulz, M., Balkanski, Y., Griesfeller, J., Prospero, J., Kinne, S., Bauer, S., Boucher, O., Chin, M., Dentener, F., Diehl, T., Easter, R., Fillmore, D., Ghan, S., Ginoux, P., Grini, A., Horowitz, L., Koch, D., Krol, M.C., Landing, W., Liu, X., Mahowald, N., Miller, R., Morcrette, J.-J., Myhre, G., Penner, J., Perlwitz, J., Stier, P., Takemura, T., Zender, C.S., 2011. Global dust model intercomparison in AeroCom phase I. Atmos. Chem. Phys. 11, 7781–7816.

Jiménez, E., Linares, C., Martínez, D., Díaz, J., 2010. Role of Saharan dust in the relationship between particulate matter and short-term daily mortality among the elderly in Madrid (Spain). Sci. Total Environ. 408 (23), 5729–5736.

Kok, J.F., Ridley, D.A., Zhou, Q., Miller, R.L., Zhao, C., Heald, C.L., Ward, D.S., Albani, S., Haustein, K., 2017. Smaller desert dust cooling effect estimated from analysis of dust size and abundance. Nat. Geosci. 10 (4), 274–278.

Kubilay, N., Saydam, A.C., 1995. Trace elements in atmospheric particulates over the eastern Mediterranean; concentrations, sources, and temporal variability. Atmos. Environ. 29, 2289–2300.

Levin, Z., Ganor, E., Gladstein, V., 1996. The effects of desert particles coated with sulfate on rain formation in the eastern Mediterranean. J. Appl. Meteorol. 35, 1511–1523.

Mandija, F., Sicard, M., Comerón, A., Alados-Arboledas, L., Guerrero-Rascado, J.L., Barragan, R., Bravo-Aranda, J.A., Granados-Muñoz, M.J., Lyamani, H., Muñoz Porcar, C., Rocadenbosch, F., Rodríguez, A., Valenzuela, A., García Vizcaíno, D., 2017. Origin and pathways of the mineral dust transport to two Spanish EARLINET sites: effect on the observed columnar and range-resolved dust optical properties. Atmos. Res. 187, 69–83.

Matthaios, V.N., Triantafyllou, A.G., Koutrakis, P., 2016. PM10 episodes in Greece: local sources versus long-range transport—observations and model simulations. J. Air Waste Manage. Assoc. 67, 105–126.

Millán, M., 2014. Extreme hydrometeorological events and climate change predictions in Europe. J. Hydrol. 518, 206–224. https://doi.org/10.1016/j.jhydrol.2013.12.041.

Millán, M., Salvador, R., Mantilla, E., Kallos, G., 1997. Photooxidant dynamics in the Mediterranean basin in summer: results from European research projects. J. Geophys. Res. 102, 8811–8824. https://doi.org/10.1029/96JD03610.

Millán, M., Mantilla, E., Salvador, R., Carratalá, A., Sanz, M.J., Alonso, L., Gangoiti, G., Navazo, M., 2000. O3 cycles in the western Mediterranean basin: interpretation of monitoring data in complex coastal terrain. J. Appl. Meteorol. 39, 487–508. https://doi.org/10.1175/1520-0450(2000)039<0487:OCITWM>2.0.CO;2.

Minguillón, M.C., Ripoll, A., Pérez, N., Prévôt, A.S.H., Canonaco, F., Querol, X., Alastuey, A., 2015. Chemical characterization of submicron regional background aerosols in the Western Mediterranean using an Aerosol Chemical Speciation Monitor. Atmos. Chem. Phys. 15, 6379–6639.

Minguillón, M.C., Pérez, N., Marchand, N., Bertrand, A., Temime-Roussel, B., Agrios, K., Szidat, S., Van Drooge, B., Sylvestre, A., Alastuey, A., Reche, C., Ripoll, A., Marco, E., Grimalt, J.O., Querol, X., 2016. Secondary organic aerosol origin in an urban environment: influence of biogenic and fuel combustion precursors. Faraday Discuss. 189, 337–359.

Mona, L., Amodeo, A., Pandolfi, M., Pappalardo, G., 2006. Saharan dust intrusions in the Mediterranean area: three years of Raman lidar measurements. J. Geophys. Res. 111, D16203. https://doi.org/10.1029/2005JD006569.

Moreno, T., Querol, X., Castillo, S., Alastuey, A., Herrmann, L., Mounkaila, M., Cuevas, E., Elvira, J., Gibbons, W., 2006. Geochemical variations in aeolian mineral particles from the Sahara–Sahel Dust Corridor. Chemosphere 65, 261–270.

Moreno, T., Pérez, N., Querol, X., Amato, F., Alastuey, A., Bhatia, R., Spiro, B., Hanvey, M., Gibbons, W., 2010. Physicochemical variations in atmospheric aerosols recorded at

sea onboard the Atlantic-Mediterranean 2008 Scholar Ship cruise (part II): natural versus anthropogenic influences revealed by PM10 trace element geochemistry. Atmos. Environ. 44, 2563–2576.
Moulin, C., Lambert, C.E., Dulac, F., Dayan, U., 1997. Control of atmospheric export of dust from N Africa by the North Atlantic Oscillation. Nature 387, 691–694.
Moulin, C., Lambert, C.E., Dayan, U., Masson, V., Ramonet, M., Bousquet, P., Legrand, M., Balkanski, Y.J., Guellel, W., Marticorena, B., Bergametti, G., Dulac, F., 1998. Satellite climatology of African dust transport in the Mediterranean atmosphere. J. Geophys. Res. 103, 13137–13144.
Pandolfi, M., Martucci, G., Querol, X., Alastuey, A., Wilsenack, F., Frey, S., O'Dowd, C.D., Dall'Osto, M., 2013. Continuous atmospheric boundary layer observations in the coastal urban area of Barcelona during SAPUSS. Atmos. Chem. Phys. 13, 4983–4996. https://doi.org/10.5194/acp-13-4983-2013 (2013).
Pandolfi, M., Tobias, A., Alastuey, A., Sunyer, J., Schwartz, J., Lorente, J., Pey, J., Querol, X., 2014a. Effect of atmospheric mixing layer depth variations on urban air quality and daily mortality during Saharan dust outbreaks. Sci. Total Environ. 494, 283–289.
Pandolfi, M., Querol, X., Alastuey, A., Jimenez, J.L., Jorba, O., Day, D., Ortega, A., Cubison, M.J., Comerón, A., Sicard, M., Mohr, C., Prévôt, A.S.H., Minguillón, M.C., Pey, J., Baldasano, J.M., Burkhart, J.F., Seco, R., Peñuelas, J., Van Drooge, B.L., Artiñano, B., Di Marco, C., Nemitz, E., Schallhart, S., Metzger, A., Hansel, H., Lorente, J., Ng, S., Jayne, J., 2014b. Effects of sources and meteorology on particulate matter in the Western Mediterranean Basin: an overview of the DAURE campaign. J. Geophys. Res. Atmos. 119, 4978–5010.
Papayannis, A., Balis, D., Amiridis, V., Chourdakis, G., Tsaknakis, G., Zerefos, C., Castanho, A.D.A., Nickovic, S., Kazadzis, S., Grabowski, J., 2005. Measurements of Saharan dust aerosols over the Eastern Mediterranean using elastic backscatter-Raman lidar, spectrophotometric and satellite observations in the frame of the EARLINET Project. Atmos. Chem. Phys. 5, 2065–2079.
Papayannis, A., Mona, L., Tsaknakis, G., Balis, D., Bösenberg, J., Chaikovski, A., De Tomasi, F., Grigorov, I., Mattis, I., Mitev, V., Müller, D., Nickovic, S., Pérez, C., et al., 2008. Systematic lidar observations of Saharan dust over Europe in the frame of EARLINET (2000–2002). J. Geophys. Res. 113, D10204. https://doi.org/10.1029/2007JD009028.
Pérez, L., Tobias, A., Querol, X., Künzli, N., Pey, J., Alastuey, A., Viana, M., Valero, N., González-Cabré, M., Sunyer, J., 2008a. Coarse particles from Saharan dust and daily mortality. Epidemiology 19 (6), 800–8007.
Pérez, N., Pey, J., Querol, X., Alastuey, A., López, J.M., Viana, M., 2008b. Partitioning of major and trace components in PM10–PM2.5–PM1 at an urban site in Southern Europe. Atmos. Environ. 42, 1677–1691.
Pérez, N., Pey, J., Castillo, S., Viana, M., Alastuey, A., Querol, X., 2008c. Interpretation of the variability of levels of regional background aerosols in the Western Mediterranean. Sci. Total Environ. 407, 527–540. https://doi.org/10.1016/j.scitotenv.2008.09.006.
Pérez, N., Pey, J., Cusack, M., Reche, C., Querol, X., Alastuey, A., Viana, M., 2010. Variability of particle number, black carbon, and PM10, PM2.5, and PM1 levels and speciation: influence of road traffic emissions on urban air quality. Aerosol Sci. Technol. 44, 487–499.
Pérez, L., Tobias, A., Querol, X., Pey, J., Alastuey, A., Diaz, J., et al., 2012. Saharan dust, particulate matter and cause-specific mortality: a case-crossover study in Barcelona (Spain). Environ. Int. 48, 150–155.
Pey, J., Querol, X., Alastuey, A., Forastiere, F., Stafoggia, M., 2013. African dust outbreaks over the Mediterranean Basin during 2001-2011: PM10 concentrations, phenomenology and trends, and its relation with synoptic and mesoscale meteorology. Atmos. Chem. Phys. 13, 1395–1410.
Prospero, J.M., Lamb, P.J., 2003. African droughts and dust transport to the Caribbean: climate change implications. Science 302, 1024–1027.
Prospero, J.M., Ginoux, P., Torres, O., Nicholson, S.E., Gill, T.E., 2002. Environmental characterization of global sources of atmospheric soil dust identified with the Nimbus 7 Total Ozone Mapping Spectrometer (TOMS) absorbing aerosol product. Rev. Geophys. 40 (1), 1002. https://doi.org/10.1029/2000RG000095.
Querol, X., Alastuey, A., Puicercus, J.A., Mantilla, E., Miro, J.V., Lopez-Soler, A., Plana, F., Artíñano, B., 1998a. Seasonal evolution of suspended particles around a large coal-fired power station: particulate levels and sources. Atmos. Environ. 32, 1963–1978.
Querol, X., Alastuey, A., Lopez-Soler, A., Plana, F., Puicercus, J.A., Ruiz, C.R., Mantilla, E., Juan, R., 1998b. Seasonal evolution of atmospheric suspended particles around a coal-fired power station: chemical characterization. Atmos. Environ. 32 (4), 719–731.
Querol, X., Alastuey, A., Rodríguez, S., Plana, F., Ruiz, C.R., Cots, N., Massagué, G., Puig, O., 2001. PM10 and PM2.5 source apportionment in the Barcelona Metropolitan Area, Catalonia, Spain. Atmos. Environ. 35/36, 6407–6419.
Querol, X., Alastuey, A., Pey, J., Pandolfi, M., Cusack, M., Pérez, N., Viana, M., Moreno, T., Mihalopoulos, N., Kallos, G., Kleanthous, S., 2009. African dust contributions to mean ambient PM10 mass-levels across the Mediterranean Basin. Atmos. Environ. 43 (28), 4266–4277.
Reche, C., Querol, X., Alastuey, A., Viana, M., Pey, J., Moreno, T., Rodríguez, S., González, Y., Fernández-Camacho, Rxt., Sánchez de la Campa, A.M., de la Rosa J., J., Dall'osto, M., Prévôt, A.S.H., Hueglin, C., Harrison, R.M., Quincey, P., 2011. New considerations for PM, black carbon and particle number concentration for air quality monitoring across different European cities. Atmos. Chem. Phys. 11, 6207–6227.
Reyes, M., Díaz, J., Tobías, A., Montero, J.C., Linares, C., 2014. Impact of Saharan dust particles on hospital admissions in Madrid. Int. J. Environ. Health Res. 24, 63–72.
Ripoll, A., Pey, J., Minguillón, M.C., Pérez, N., Pandolfi, M., Querol, X., Alastuey, A., 2014. Three years of aerosol mass, black carbon and particle number concentrations at Montsec (southern Pyrenees, 1570 m a.s.l.). Atmos. Chem. Phys. 14, 4279–4295. https://doi.org/10.5194/acp-14-4279-2014.
Ripoll, A., Minguillón, M.C., Pey, J., Pérez, N., Querol, X., Alastuey, A., 2015. Joint analysis of continental and regional background environments in the western Mediterranean: PM1 and PM10 concentrations and composition. Atmos. Chem. Phys. 15 (2), 1129–1145. https://doi.org/10.5194/acp-15-1129-2015.
Rodriguez, S., Querol, X., Alastuey, A., Kallos, G., Kakaliagou, O., 2001. Saharan dust inputs to suspended particles time series (PM10 and TSP) in Southern and Eastern Spain. Atmos. Environ. 35 (14), 2433–2447.
Rodríguez, S., Querol, X., Alastuey, A., Kallos, G., Kakaliagou, O., 2001. Saharan dust contributions to PM10 and TSP levels in Southern and Eastern Spain. Atmos. Environ. 35, 2433–2447.
Rodríguez S., A. Alastuey, S. Alonso-Pérez, X. Querol, E. Cuevas, J. Abreu-Afonso, M. Viana, M. Pandolfi, And J. De La Rosa., 2011. Transport of desert dust mixed with N African industrial pollutants in the subtropical Saharan Air Layer. Atmos. Chem. Phys., 11, 6663–6685.
Rolph, G., Stein, A., Stunder, B., 2017. Real-time environmental applications and display sYstem: READY. Environ. Model Softw. 95, 210–228.
Salvador, P., Artíñano, B., Molero, F., Viana, M., Pey, J., Alastuey, A., Querol, X., 2013. African dust contribution to ambient aerosol levels across central Spain: characterization of long-range transport episodes of desert dust. Atmos. Res. 127, 117–129.
Salvador, P., Alonso, S., Pey, J., Artíñano, B., de Bustos, J.J., Alastuey, A., Querol, X., 2014. African dust outbreaks over the western Mediterranean basin: 11 year characterization of atmospheric circulation patterns and dust source areas. Atmos. Chem. Phys. 14, 6759–6775. https://doi.org/10.5194/acp-14-6759-2014.
Salvador, P., Almeida, S.M., Cardoso, J., Almeida-Silva, M., Nunes, T., Cerqueira, M., Alves, C., Reis, M.A., Chaves, P.C., Artíñano, B., Pio, C., 2016. Composition and origin of PM10 in Cape Verde: characterization of long-range transport episodes. Atmos. Environ. 127, 326–339.
Stein, A.F., Draxler, R.R., Rolph, G.D., Stunder, B.J.B., Cohen, M.D., Ngan, F., 2015. NOAA's HYSPLIT atmospheric transport and dispersion modelling system. Bull. Amer. Meteor. Soc. 96, 2059–2077.
Textor, C., Schulz, M., Guibert, S., Kinne, S., Balkanski, Y., Bauer, S., Berntsen, T., Berglen, T., Boucher, O., Chin, M., Dentener, F., Diehl, T., Easter, R., Feichter, H., Fillmore, D., Ghan, S., Ginoux, P., Gong, S., Grini, A., Hendricks, J., Horowitz, L., Huang, P., Isaksen, I., Iversen, I., Kloster, S., Koch, D., Kirkevåg, A., Kristjansson, J.E., Krol, M., Lauer, A., Lamarque, J.F., Liu, X., Montanaro, V., Myhre, G., Penner, J., Pitar, G., Reddy, S., Seland, Ø., Stier, P., Takemura, T., Tie, X., 2006. Analysis and quantification of the diversities of aerosol life cycles within AeroCom. Atmos. Chem. Phys. 6, 1777–1813.
Tobías, A., Pérez, L., Díaz, J., Linares, C., Pey, J., Alastruey, A., Querol, X., 2011. Short-term effects of particulate matter on total mortality during Saharan dust outbreaks: a case-crossover analysis in Madrid (Spain). Sci. Total Environ. 412–413, 386–389.
Varga, G., 2012. Spatio-temporal distribution of dust storms—a global coverage using NASA TOMS aerosol measurements. Hung. Geogr. Bull. 61, 275–298.
Viana, M., Querol, X., Alastuey, A., Cuevas, E., Rodríguez, S., 2002. Influence of African dust on the levels of atmospheric particulates in the Canary Islands air quality network. Atmos. Environ. 36 (38), 5861–5875.
Walker, A.L., Liu, M., Miller, S.D., Richardson, K.A., Westphal, D.L., 2009. Development of a dust source database for mesoscale forecasting in southwest Asia. J. Geophys. Res. 114, D18207. https://doi.org/10.1029/2008JD011541.
Washington, R., Todd, M., Middleton, N., Goudie, A.S., 2003. Global dust storm source areas determined by the Total Ozone Monitoring Spectrometer and ground observations. Ann. Assoc. Am. Geogr. 93, 297–313.